⌘ *Author's Choice*

THE JOURNAL OF BIOLOGICAL CHEMISTRY VOL. 284, NO. 23, pp. 15573–15588, June 5, 2009

Separate Elements within a Single IQ-like Motif in Adenylyl Cyclase Type 8 Impart Ca^{2+}/Calmodulin Binding and Autoinhibition*[S]

Received for publication, December 19, 2008, and in revised form, March 6, 2009 Published, JBC Papers in Press, March 21, 2009, DOI 10.1074/jbc.M809585200

David A. MacDougall[‡], Sebastian Wachten[‡], Antonio Ciruela[‡], Andrea Sinz[§], and Dermot M. F. Cooper[‡1]

From the [‡]Department of Pharmacology, University of Cambridge, Tennis Court Road, Cambridge CB2 1PD, United Kingdom and the [§]Institute of Pharmacy, Martin Luther University Halle-Wittenberg, Wolfgang-Langenbeck-Strasse 4, D-06120 Halle (Saale), Germany

The ubiquitous Ca^{2+}-sensing protein calmodulin (CaM) fulfills its numerous signaling functions through a wide range of modular binding and activation mechanisms. By activating adenylyl cyclases (ACs) 1 and 8, Ca^{2+} acting via calmodulin impacts on the signaling of the other major cellular second messenger cAMP. In possessing two CaM-binding domains, a 1-5-8-14 motif at the N terminus and an IQ-like motif (IQ*lm*) at the C terminus, AC8 offers particularly sophisticated regulatory possibilities. The IQ*lm* has remained unexplored beyond the suggestion that it bound CaM, and the larger C2b region of which it is part was involved in the relief of autoinhibition of AC8. Here we attempt to distinguish the function of individual residues of the IQ*lm*. From a complementary approach of *in vitro* and cell population AC activity assays, as well as CaM binding, we propose that the IQ*lm* alone, and not the majority of the C2b, imparts CaM binding and autoinhibitory functions. Moreover, this duality of function is spatially separated and depends on amino acid side-chain character. Accordingly, residues critical for CaM binding are positively charged and clustered toward the C terminus, and those essential for the maintenance of autoinhibition are hydrophobic and more N-terminal. Secondary structure prediction of the IQ*lm* supports this separation, with an ideally placed break in the α-helical nature of the sequence. We additionally find that the N and C termini of AC8 interact, which is an association specifically abrogated by fully Ca^{2+}-bound, but not Ca^{2+}-free, CaM. These data support a sophisticated activation mechanism of AC8 by CaM, in which the duality of the IQ*lm* function is critical.

The divalent calcium ion, Ca^{2+}, plays a key role in modulating cellular processes as diverse as fertilization and apoptosis (1, 2). Ca^{2+} concentrations inside the cell are held ~100 nM, despite a perpetually higher level of 1–2 mM in the extracellular medium. This steep gradient across the plasma membrane allows for a large influx when Ca^{2+} channels open, with subsequent signaling events that often rely on transduction via Ca^{2+}-binding proteins (3). The archetypal Ca^{2+} sensor is calmodulin (CaM),[2] a small, acidic protein so strictly conserved that all vertebrate CaM genes encode an identical 148-residue sequence (4). Multifunctional in its downstream effects, CaM can bind to at least 300 target proteins with novel partners continuing to be discovered (5). The list of effectors includes two isoforms of the adenylyl cyclase (AC) superfamily, AC1 and AC8, which comprise the Ca^{2+}-stimulable subset of the nine particulate ACs (6). In intact cells, AC8 exhibits a predilection for store-operated, or capacitative, Ca^{2+} entry (CCE) (7, 8). This mode of Ca^{2+} entry is triggered by the emptying of endo/sarcoplasmic reticular stores by physiological or pharmacological stimuli (9, 10). Although the mechanism of the regulation of AC8 in nonexcitable cells by CCE (or voltage-gated Ca^{2+} entry in neurons) can be viewed to rely on facets of cellular compartmentalization (11–13), the detailed molecular mechanism whereby Ca^{2+} stimulates the enzyme is unclear. Consequently, the present investigation addresses the molecular mechanism whereby Ca^{2+}, acting via calmodulin, stimulates AC8.

The broad features of CaM that hold the key to its multiple regulatory strategies are understood. CaM is organized into two homologous globular domains (or lobes) united by a short linker segment (14). Both the N-terminal (N-lobe) and the C-terminal lobe (C-lobe) include two EF-hands (specialized Ca^{2+}-coordinating helix-loop-helix motifs (15)), endowing CaM with four Ca^{2+}-binding sites. Ca^{2+} binding to either lobe of CaM induces a structural reconfiguration determined by the two helices of each EF-hand separating from near-antiparallel to perpendicular arrays (14, 16). This exposes hydrophobic trenches in the C- and N-lobes sequentially (because the former has the highest affinity for Ca^{2+}), which are notably lined with a disproportionate number of flexible methionine side chains, ready to accommodate a remarkable array of unrelated sequences. Initially, the mode of Ca^{2+}-loaded CaM association with targets was considered to be uniform; the N- and C-lobes collapsed around the target peptides of *e.g.* smooth muscle myosin light chain kinase (17), skeletal muscle myosin light chain kinase (18), and CaMKIIα (19) with the N-lobe favoring

* This work was supported by Wellcome Trust Grant RG31760.
⌘ *Author's Choice*—Final version full access.
[S] The on-line version of this article (available at http://www.jbc.org) contains supplemental "Experimental Procedures," "Results," Table 1, and Figs. 1–7.
[1] Royal Society Wolfson Research Fellow. To whom correspondence should be addressed. Tel.: 44-1223-334063; Fax: 44-1223-334040; E-mail: dmfc2@cam.ac.uk.

[2] The abbreviations used are: CaM, calmodulin; AC, adenylyl cyclase; $AC8_{38-40,49-51ala}$, AC8 N-terminal CaM-binding mutant; CaMBD, CaM-binding domain; CCE, capacitative Ca^{2+} entry; CEC, concentration-effect curve; IQ*lm*, IQ-like motif; FSK, forskolin; GST, glutathione *S*-transferase; MBP, maltose-binding protein; TG, thapsigargin; WT, wild-type; TBS, Tris-buffered saline; PBS, phosphate-buffered saline; ANOVA, analysis of variance.

the C-terminal target sequence and vice versa. However, CaM has since proven to be more versatile and unpredictable in how it associates with and regulates effectors, with reports of N-lobe-N-terminal/C-lobe-C-terminal interaction (20), target dimerization promoted by CaM (21), CaM binding to fatty acyl modifications (22), and other deviations from the early model.

Nevertheless, three main forms of CaM regulation have been proposed as follows: relief of autoinhibition; active site remodeling; and dimerization of target domains (23). Whether the precise mechanism of CaM binding and subsequent regulation of AC8 falls into these categories of CaM regulation is not resolved. A previous study (24) established that AC8 possesses two calmodulin-binding domains (CaMBDs). CaM recognition sequences generally show little homology, although classifications based on relative positions of key hydrophobic residues have been usefully applied (4). The N-terminal CaMBD of AC8 conforms to a "1-5-8-14 motif" having large hydrophobic side chains from Trp, Val, or Ile residues at these spatially conserved sites. The C-terminal CaMBD contains an IQ-like motif (IQ*lm*), in accordance with a signature (IVL)Q*XXX*R(K) arrangement, to which CaM binds directly (25). By truncating one terminus or both termini, Gu and Cooper (24) asserted that the N terminus contributed little to direct CaM regulation of AC8, whereas the C terminus was critical for the maintenance of an auto-inhibited state, which was relieved upon binding of CaM. Thus, functional elements of both autoinhibition and pre-association, imparted by noncontiguous CaMBDs, have been suggested, thereby excluding AC8 from a simple model of CaM binding to an autoinhibitory domain leading to activation, as is sometimes observed (23).

Recently, the proposal that the two CaMBDs play separate roles in AC8 activation was reinforced (26). This study suggested that CaM tethering by the N-terminal 1-5-8-14 motif provides the catalytically relevant C-terminal CaMBD with privileged access to CaM, thereby circumventing the need for AC8 to compete for CaM, whose free concentration in the cell is far exceeded by that of its targets (27, 28). 1–14 motifs are more generally employed in relieving autoinhibitory influences (23), so the use by AC8 of a 1-5-8-14 motif as a CaM-tethering site is unusual. The proposal that CaM pre-associates here was based on limited mutagenesis of residues within the 1-5-8-14 motif of AC8 and the use of CaM mutants whose Ca^{2+} binding capability was abolished completely or limited to discrete lobes. In contrast to the 1-5-8-14 motif at the N terminus, very little is known of the IQ*lm* at the C terminus, in terms of the roles of the individual residues in CaM binding or autoinhibition, or even on the interplay between CaMBDs at the N and C termini of AC8.

Against this background, the present study sought to assess the contribution of IQ*lm* residues to the function of AC8, focusing on consequences of key mutations on CaM-binding efficiency, regulation by Ca^{2+}/CaM, and maintenance of the autoinhibited state. Through this series of experiments, the level of coordination between the IQ-like and 1-5-8-14 motifs became evident. The provision of a pre-associated CaM molecule was found to allow for potentially deleterious mutations of the IQ*lm* to be tolerated. Within this latter motif, Leu^{1196}, Val^{1197}, and Leu^{1200} are residues essential to autoinhibition, whereas the main responsibility of binding CaM directly at the C terminus lies with Arg^{1202} and Arg^{1204}. In this regard, the AC8 IQ*lm* spatially separates the two functions of CaM binding and maintenance of autoinhibition, a separation that is supported by a predicted break in the helicity of the IQ*lm* region. Thus, a new variation is revealed in the manner by which a target exploits the CaM device into a sophisticated activation mechanism.

EXPERIMENTAL PROCEDURES

Materials—All materials were purchased from Sigma with exceptions as noted. Forskolin (FSK) and thapsigargin (TG) were purchased from Merck. [2-^{3}H]Adenine, [2,8-^{3}H]cAMP, [α-^{32}P]ATP, enhanced chemiluminescence (ECL) Western blotting analysis system, and horseradish peroxidase-conjugated goat anti-rabbit IgG were obtained from GE Healthcare. Fura-2 free acid and fura-FF free acid were from Invitrogen. Protein molecular weight standards and acrylamide/bisacrylamide 37.5:1 solution were from Bio-Rad. DNA T4 ligase, calf intestinal phosphatase, and monoclonal antibody raised against MBP were from New England Biolabs (Ipswich, MA). Horseradish peroxidase-conjugated goat anti-mouse IgG was from Promega (Madison, WI). Re-blot plus strong solution (10×) was obtained from Chemicon (Temecula, CA). The polyclonal AC8 antibody was generously supplied by J. J. Cali (Promega Corp., Madison, WI), and the monoclonal anti-CaM antibody was obtained from Millipore Corp. (Billerica, MA). Lobe-specific Ca^{2+}-binding mutant CaM constructs were a gift from J. H. Caldwell (University of Colorado Health Sciences Center, Denver, CO). Oligonucleotides were from Sigma Genosys.

Plasmid cDNA Production—Wild-type rat CaM cDNA was inserted into the pQE30 vector as described recently (26). pGEX4T1–8Ct was produced as detailed elsewhere (26). A cDNA fragment encoding the first 179 residues of the protein was amplified by PCR using the following primers, (5′ to 3′) GGGAGCTCATGGAACTCTCGGATGTGCACTGC (5′) and CGCGTCGACTTACTCCGATTTGCGCCTCTGG (3′), and subcloned into pMALp4G plasmid using the appropriate restriction enzymes, SacI (5′) and SalI (3′). Amino acid substitution mutants of AC8 were produced by site-directed mutagenesis, using the QuikChange® kit (Stratagene, La Jolla, CA). C-terminal truncation mutants were produced via a PCR-based strategy, using AC8 internal EcoRV and XbaI sites, by 5′ and 3′ primers, respectively. A table detailing the primers used to generate 11 IQ*lm* and four truncation mutants is provided in supplemental Table 1. $AC8_{38-40,49-51ala}{}^{VQR/AAA}$ was created by using the same primers as for $AC8^{VQR/AAA}$ but starting with $AC8_{38-40,49-51ala}$ (26) as template.

Purification of Rat His$_6$-CaM—XL10 Gold *Escherichia coli* cells, transformed with wild-type or mutant rat CaM pQE30 plasmids, were grown at 37 °C with vigorous agitation until the absorbance at 600 nm (A_{600}) reached ~0.8. Expression of the His$_6$-tagged CaM was then induced with 1 mM isopropyl β-D-thiogalactopyranoside and maintained for 6 h. Cell suspensions were centrifuged at 6000 × *g*, 4 °C for 15 min, and the supernatant was discarded and the resulting pellet resuspended in cell disruption buffer (140 mM NaCl, 20 mM Tris, pH 7.8, 1 mM phenylmethylsulfonyl fluoride, and 1 mM benzamidine).

Lysates were produced by passing the sample twice through a constant cell disruption apparatus (Constant Cell Systems, Daventry, UK). After lysis, samples were heated to 65 °C for 10 min and then centrifuged at 16,000 × *g* for 20 min at 4 °C to sediment cell debris and insoluble endogenous protein aggregates. His_6-CaM was then purified using immobilized metal ion affinity chromatography (TALON®, Clontech).

Generation of GST and GST Fusion Protein Glutathione-Sepharose Matrices—The expression of GST, GST-8Ct, GST-8C2b, and GST-8C2b mutant proteins in BL21 (DE3) cells for 3 h at 30 °C was induced with 0.1 mM isopropyl β-D-thiogalactopyranoside. Cells were lysed by sonication in lysis buffer (PBS supplemented with 1 mM benzamidine, 1 mM phenylmethylsulfonyl fluoride, 10 μM EDTA, and 1 ng of DNase). Homogenates were then centrifuged at 16,000 × *g* for 15 min at 4 °C, and the pellet discarded. The supernatant fraction was passed through glutathione-Sepharose resin by chromatography and washed until no protein remained in the eluate (assessed by absorbance at 280 nm). A volume of PBS equal to the resin volume was used to create 50% slurry, to which 0.02% (v/v) NaN_3 was added.

Preparation of MBP-8Nt-containing Soluble Bacterial Lysates—BL21 (DE3) cells transformed with pMALp4G-8Nt1 plasmids were cultured, and expression of MBP-8Nt was instigated by treatment with 0.1 mM isopropyl β-D-thiogalactopyranoside for 3 h at 30 °C. Lysis was performed as described above under "Generation of GST and GST Fusion Protein Glutathione-Sepharose Matrices." Supernatant fractions were snap-frozen on dry ice before storage at −80 °C.

Cell Culture and Transfection of HEK293 Cells—HEK293 cells (European Collection of Cell Cultures, Porton Down, UK) were grown in minimum essential medium with Earle's salts, supplemented with 10% (v/v) fetal bovine serum, 2 mM L-glutamine, 50 μg/ml penicillin, 50 μg/ml streptomycin, and 100 μg/ml neomycin. Cultures were maintained at 37 °C in a humidified atmosphere of 95% air and 5% CO_2. Transient transfection of wild-type and mutant AC8 was achieved using the calcium phosphate method (29). Cells were passaged such that 30–40% confluence was reached on the day of transfection. An 8-h incubation with transfection material was standard. For cell population studies, transfected cultures were seeded into 24-well plates for 24 h, and assay was performed 48 h post-transfection. For *in vitro* AC assays, crude membrane fractions were extracted, as described previously (26), 48 h after transfection.

In Vitro Measurement of Adenylyl Cyclase Activity—Determination of adenylyl cyclase activity *in vitro* was performed as detailed elsewhere (30), with some modifications. Free Ca^{2+} concentrations were established from a series of $CaCl_2$ solutions buffered with 200 μM EGTA, based on the BAD4 program (31) and confirmed by spectrofluorometric measurements with fura-2 and fura-FF as described previously (26). [^{3}H]cAMP (~6000 cpm) was added as a recovery marker, and the [^{32}P]cAMP formed was quantified using a sequential chromatography technique described previously (32).

Measurement of cAMP Accumulation in Cell Populations—cAMP accumulation in intact cells was measured according to the method of Evans *et al.* (33), with some modifications as described previously (26). Transfected HEK293 cells were incubated in minimal essential medium with [2-^{3}H]adenine (1.5 μCi/well in 24-well plates) at 37 °C for 90 min to radiolabel the ATP pool. To observe the effect of CCE, cells were preincubated for 4 min with 100 nM TG in the presence of EGTA and isobutylmethylxanthine, and cAMP accumulation was measured over a 1-min period beginning with the addition of various concentrations of $CaCl_2$ and 10 μM FSK. Both the [^{3}H]ATP and [^{3}H]cAMP content were quantified, following sequential chromatography. Accumulation of cAMP is expressed as the percentage conversion of [^{3}H]ATP into [^{3}H]cAMP.

GST Pulldown Assays—For pulldown assays assessing CaM binding to GST, GST-8C2b, and GST-8C2b mutants, glutathione-Sepharose 4B supporting the appropriate immobilized GST or GST fusion was added to PBS supplemented with 0.1% Triton X-100 (v/v), 0.5 μM His_6-CaM, and 20 μM $CaCl_2$. Samples were rotated for 2 h at 4 °C, centrifuged (19,000 × *g*, 5 min, 4 °C), and washed three times in PBS. This was followed by SDS-PAGE analysis and Western blotting with CaM, AC8, and GST antibodies, as detailed below (see under "Immunoblotting"). For GST-8Ct/GST-8C2b pulldown of MBP-8Nt from bacterial lysates, the procedure was identical, except supernatant fractions from bacterial lysis were used in place of PBS as the starting medium.

Immunoblotting—Procedures were performed at room temperature unless stated otherwise. Proteins were resolved using discontinuous SDS-PAGE with a 5% acrylamide stacking gel and a 10, 12, or 15% acrylamide separating gel. Separated proteins were then transferred to a supported nitrocellulose membrane. After transfer, nitrocellulose membranes were optionally washed in Ponceau stain to visualize protein and then blocked for 1 h in TBS (20 mM Tris, pH 7.5, 150 mM NaCl) containing 5% nonfat dried milk. Membranes were incubated with anti-GST (1:50,000) or anti-MBP (1:50,000) for 30 min, or anti-CaM (1:5000) or anti-AC8 (1:5000) for 1 h, in TTBS (TBS plus 0.1% Tween 20) containing 1% nonfat dried milk. Membranes were washed (three times for 5 min) in TTBS and then incubated with goat anti-mouse IgG (after monoclonal CaM, GST, and MBP primary antibodies) conjugated to horseradish peroxidase (1:10,000 dilution of stock) or goat anti-rabbit IgG (for polyclonal AC8 primary antibody) conjugated to horseradish peroxidase (1:10,000) in TTBS plus 1% nonfat dried milk for 30 min (GST, MBP) or 1 h (CaM, AC8). Finally, the membranes were washed three times in TTBS (5 min), once in TBS, and subjected to ECL, in accordance with the manufacturer's guidelines. When required, after the first ECL stage, membranes were stripped using Re-blot Plus Strong solution according to the manufacturer's protocol, blocked again in TBS containing 5% nonfat dried milk, and re-probed using the same procedure described above.

Curve Fitting and Statistical Analyses—Sigmoidal dose-response curves were obtained using GraphPad Prism version 4 (GraphPad Software Inc.). Data points of representative experiments are shown as means ± S.D. of triplicate determinations. Mean maximal Ca^{2+}/CaM stimulation of three or more experiments are expressed as mean ± S.E. Statistical significance of differences in mean maximal stimulation between AC8 and $AC8_{\Delta 1-106}$ IQ*lm* mutants was assessed with unpaired *t* tests. One-way ANOVAs were used where appropriate, followed by

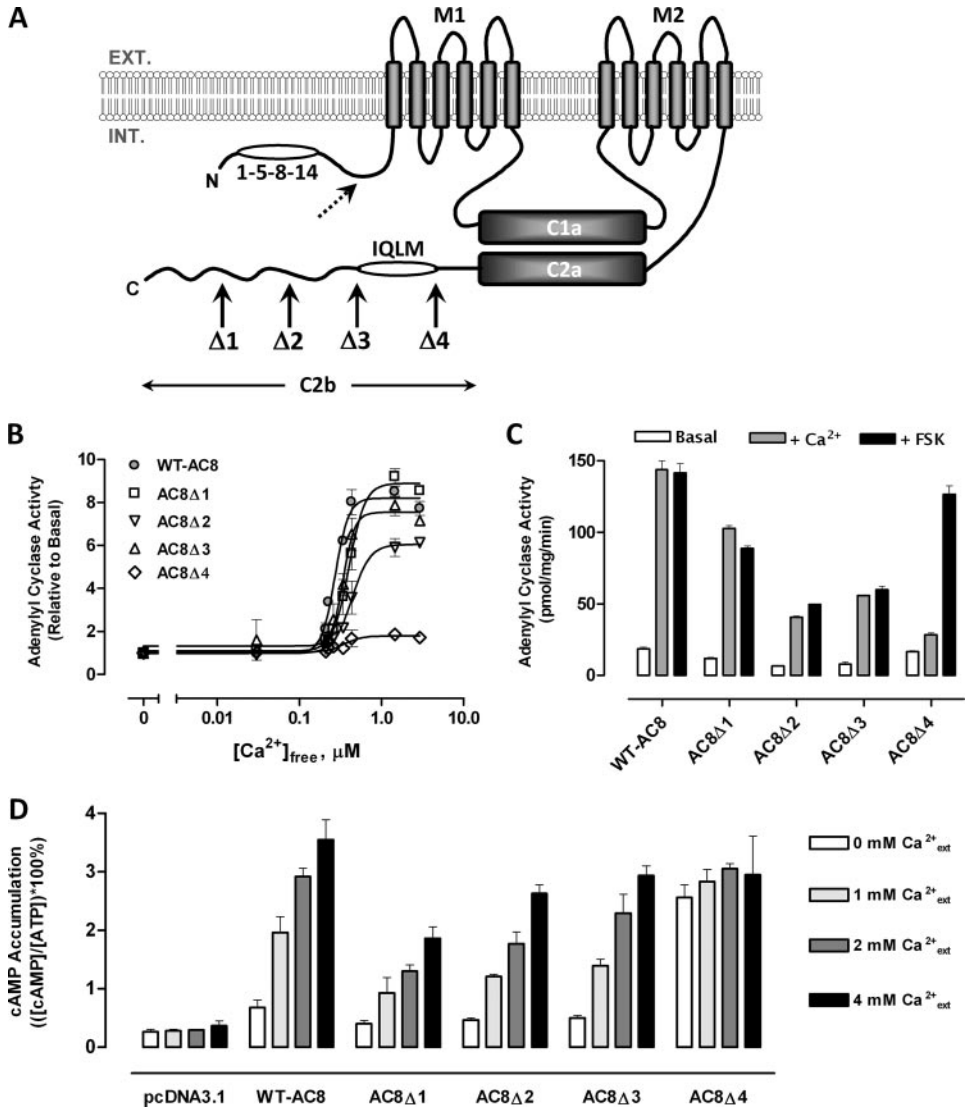

FIGURE 1. **The C-terminal CaMBD and autoinhibitory domain of AC8 are both contained within the same 24-residue sequence.** *A*, schematic representation of AC domains. *M1* and *M2* denote transmembrane cassettes 1 and 2, which, together with C1a and C2a, are homologous among all ACs. C1a and C2a interact to form a catalytic dimer. The N terminus and C2b domains, as well as the region linking C1a and M2, C1b, are more heterogeneous within the AC superfamily and impart isoform-specific regulation. Accordingly, AC8 has one CaMBD at the N terminus (1-5-8-14) and in the C2b domain (IQ*lm*). *Arrows* indicate the sites of truncation in four deletion mutants as follows: AC8Δ1, residues 1237–1248 deleted; AC8Δ2, 1225–1248 deleted; AC8Δ3, 1213–1248 deleted; and AC8Δ4, 1197–1248 deleted. The *dashed arrow* indicates the truncation point of the N-terminal mutant, AC8Δ1–106 (see Fig. 2). *B,* AC activity in crude membranes from HEK293 cells transiently transfected with cDNA encoding rat wild-type (*WT*) AC8 or one of four truncation mutants. Activity is normalized to the basal level in the absence of Ca^{2+}. *C,* basal activity is compared with Ca^{2+} (1 μM) and FSK (10 μM) regulated activity. *D,* CCE-evoked AC activity of vector (pcDNA3), WT-AC8, and truncation mutant transfected HEK293 cell population assays.

Dunnett's or Newman-Keuls multiple comparisons tests, where $p < 0.05$ (*) and $p < 0.01$ (**) were considered significant.

RESULTS

Serial Truncation of the AC8 C Terminus Reveals a Shared Boundary of Autoinhibitory and Calmodulin-binding Domains—The gross domain topology of AC8 is schematized in Fig. 1*A*. The C2b region of AC8 performs at least three functions, including binding of CaM, allowing subsequent regulation by CaM, and maintenance of autoinhibition. Whether or how these functions are divided within the C-terminal sequence is unknown. Earlier truncation experiments had concluded that the main autoinhibitory element of AC8 lies between residues 1184 and 1248 (24). Because the IQ*lm*, potentially important in regulation by CaM, lies between residues Val^{1197} and Asn^{1212}, we wondered whether an autoinhibitory domain might follow in the subsequent C-terminal sequence. Hence, four truncation mutants were generated as follows: the first three representing successive 12 amino acid deletions from the C terminus, and the final one also truncating the entire IQ-like motif. *Arrows* on the schematic diagram of AC8 in Fig. 1*A* at the C2b region indicate truncation points of the four numbered mutants. Mutant cDNAs were transiently transfected into HEK293 cells, from which crude membrane fractions were extracted, and *in vitro* AC activity was assessed in the presence of 1 μM CaM and varying concentrations of $Ca^{2+}{}_{free}$. Fig. 1*B* shows a representative data set from three such experiments and demonstrates the Ca^{2+}/CaM stimulation of AC8Δ1, AC8Δ2, and AC8Δ3 to be analogous to that of wild-type AC8. As reported previously, Ca^{2+}-stimulated WT-AC8 activity in this heterologous system is usually from 5- to 11-fold over basal (26). Aggregated maximal stimulation by Ca^{2+}/CaM shows that WT-AC8, AC8Δ1, AC8Δ2, and AC8Δ3 all display activation in this range (8.3 ± 2.0, 7.6 ± 3.1, 8.3 ± 3.4, and 7.2 ± 2.1; mean ± S.E.), but AC8Δ4 falls dramatically short of the lower limit (1.5 ± 0.2). By one-way analysis of variance, AC8Δ4 is the only mutant to significantly differ from WT-AC8 (supplemental Fig. 1*A*). However, activity of the AC8Δ4 is not eliminated, because robust FSK-induced stimulation, comparable with that of WT, is still observed (Fig. 1*C*). When the Ca^{2+} stimulation of WT and mutant ACs is expressed as a percentage of FSK activity over three experiments, AC8Δ4 is the only mutant to be significantly compromised (supplemental Fig. 1*B*).

Although the *in vitro* assay used above allows us to examine directly the effect of prescribed Ca^{2+} and CaM concentrations on AC/mutant activity, intact cell cAMP accumulation measurement provide information from a more physiological context, where [CaM] is limiting. Thus, the truncation mutants were also assessed in cell populations for their response to CCE,

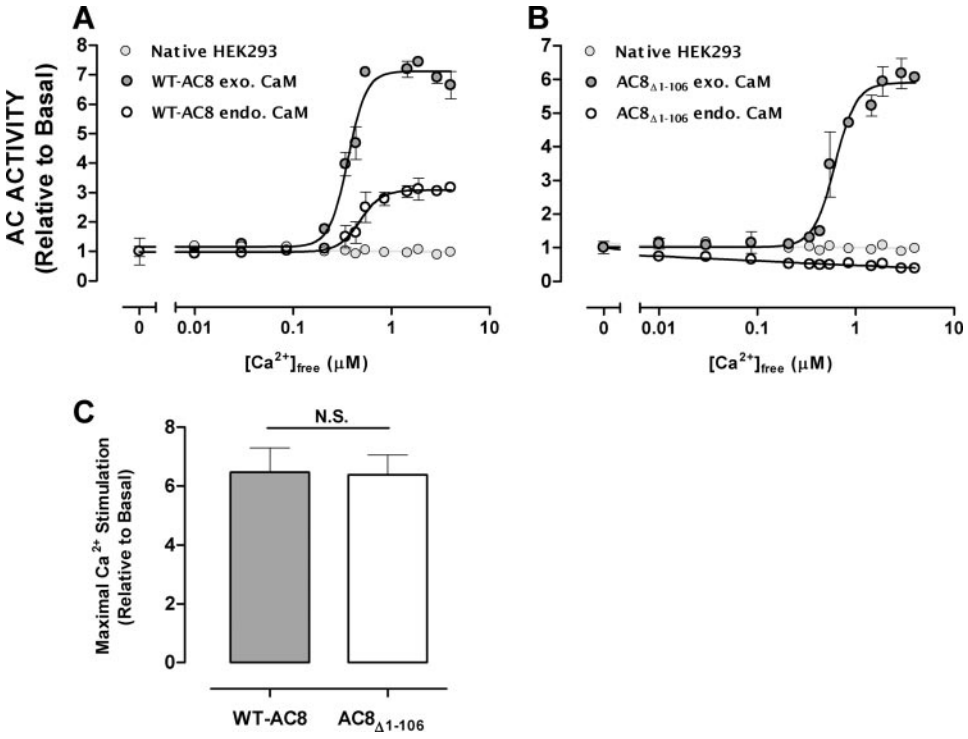

FIGURE 2. ***In vitro*, WT-AC8 and AC8$_{\Delta 1-106}$ are functionally equivalent in the presence of exogenous CaM.** *A*, crude membranes prepared from HEK293 cells transiently transfected with cDNA encoding rat WT-AC8 respond to increasing $[Ca^{2+}]_{free}$ in the presence of both endogenous and exogenous CaM. *B*, under the same experimental conditions, AC8$_{\Delta 1-106}$ is activated by Ca^{2+} in the presence of exogenous CaM at 1 μM to a similar level as WT-AC8. In the absence of exogenous CaM, AC8$_{\Delta 1-106}$ is, in contrast to WT-AC8, not activated by Ca^{2+}. *C*, maximal Ca^{2+} stimulation in the presence of 1 μM CaM is not statistically different between WT-AC8 (6.47 $\pm$ 0.83; mean $\pm$ S.E., $n = 11$) and AC8$_{\Delta 1-106}$ (6.39 $\pm$ 0.67; mean $\pm$ S.E., $n = 6$) when compared using an unpaired *t* test. *N.S.*, not significant.

the mode of Ca^{2+} entry to which AC8 preferentially responds. CCE was triggered by pretreatment with EGTA and the sarco/endoplasmic reticulum Ca^{2+}-ATPase inhibitor TG. Subsequent application of $CaCl_2$ to the extracellular medium initiated CCE (exemplar traces depicting the resultant $[Ca^{2+}]_i$ rise(s) in supplemental Fig. 2*A*). Having pre-labeled the ATP pool with [^{3}H]adenine, accumulation of radiolabeled cAMP could be quantified. Fig. 1*D* shows a representative data set, where the robust stimulation typical of AC8-transfected cells contrasts with a lack of Ca^{2+} activation observed in empty vector-transfected cells. Although the absolute levels of activity varied somewhat, the stimulation profiles of AC8Δ1, AC8Δ2, and AC8Δ3 closely match that of WT-AC8 in terms of the graded increases in cAMP accumulation in response to increasing external Ca^{2+} and the ratio of basal to maximal activity. Again, AC8Δ4 stood apart from the other truncation mutants; a strikingly high basal activity was observed, which was refractory to further stimulation by Ca^{2+}. These data, together with the *in vitro* data, allowed us to conclude that residues 1197–1212 are required for both Ca^{2+} stimulation and maintenance of autoinhibition. Very curiously, we did note that AC8Δ4 retained a small degree of stimulation by Ca^{2+} both *in vitro* and *in vivo*. Concerned that residues N-terminal to Val^{1197} might contribute to Ca^{2+}/CaM regulation, we compared AC8Δ4 with a more severe truncation mutant, AC8Δ5 (truncated from residue 1184), and we found that it too responded slightly to Ca^{2+} in cell population assays (supplemental Fig. 2*B*). Because Pro^{1184} marks the C-terminal limit of the catalytic C1a domain, further truncation is not practical, and we must conclude that although Ca^{2+}/CaM stimulation is almost exclusively imparted by the C2b region (1184–1248), CaM contributed by the N terminus can activate AC8 to a very minor extent.

Truncation of the AC8 N Terminus Does Not Affect Exogenous Ca^{2+}/CaM Stimulation in Vitro—Previous experiments indicated only a marginal contribution of the N terminus to stimulation by Ca^{2+}/CaM of AC8 (11, 24, 26), because deletion of the first 106 amino acids (referred to henceforth as AC8$_{\Delta 1-106}$) did not affect *in vitro* stimulation of the enzyme. A *dashed arrow* at the N terminus of the schematic in Fig. 1*A* indicates the truncation point of AC8$_{\Delta 1-106}$. As a prelude to more detailed analysis of the IQ*lm*, it is shown in Fig. 2 that both AC8 and AC8$_{\Delta 1-106}$ display robust Ca^{2+}/CaM stimulation of activity and also that the level of stimulation achieved by 1 μM CaM is not statistically separable over multiple assays ($p < 0.05$, Fig. 2*C*). Indeed, the activities were almost identical (6.47 $\pm$ 2.78 and 6.39 $\pm$ 1.64 maximal Ca^{2+} stimulation relative to basal) for AC8 and AC8$_{\Delta 1-106}$, respectively. EC_{50} values for Ca^{2+} were congruent with those previously published (26), with EC_{50} values of AC8$_{\Delta 1-106}$ being slightly higher than WT-AC8 at 0.61 and 0.36 μM, respectively, in the presence of exogenous CaM. A moderate level of stimulation (~2.5–3-fold) persists after EGTA washing, in the absence of added CaM, with AC8, but not with AC8$_{\Delta 1-106}$. This reflects the likely pre-association of CaM at the N terminus of AC8 (26). Nevertheless, in the presence of exogenous CaM, the two enzymes are indistinguishable in their response to Ca^{2+}.

Mutation of IQlm Residues Does Not Affect Ca^{2+} Regulation of Full-length AC8 in Vitro—Having established that AC8 and AC8$_{\Delta 1-106}$ are functionally equivalent in the *in vitro* situation, we generated point mutations in the IQ*lm* of AC8. This sequence is defined by the presence of an IQ-like motif, conforming to the signature (V/I/L)Q*XXX*R(K) pattern, ^{1196}L**VQ**SLN**R**QRQKQLLNE^{1211}. We began by making single substitutions of consensus IQ*lm* residues in which the substituted side chains were of comparable size to those they replaced (V1197N, Q1198K, and R1202Q). Two of these were combined to produce V1197N/R1202Q. More severely, the first two and then all three consensus IQ*lm* amino acids were replaced with alanine to yield V1197A/Q1198A and V1197A/Q1198A/R1202A. Two resident arginines, and separately the sole lysine, were charge-reversed to glutamate (R1202/R4E and K1206E). A pair of prox-

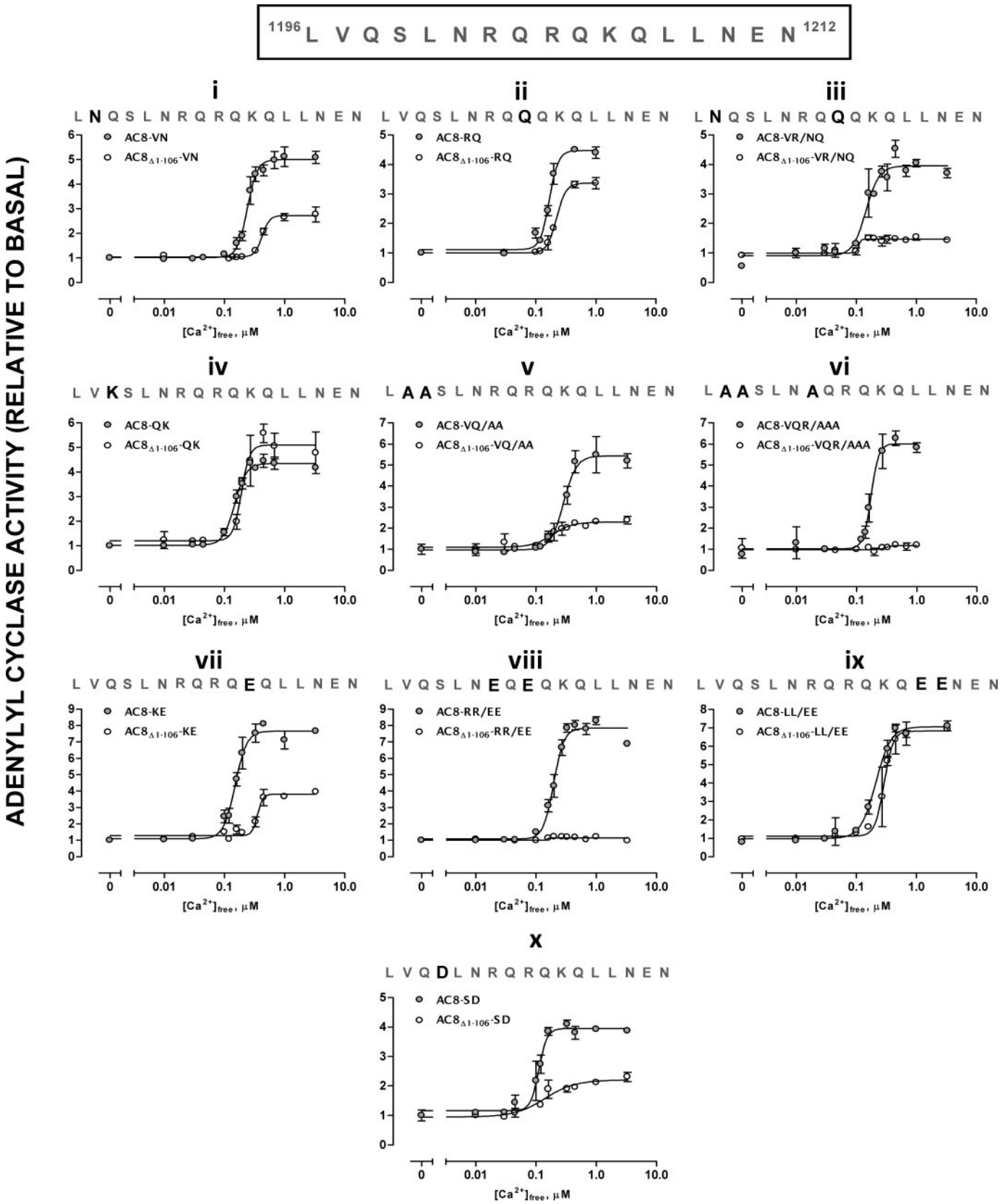

FIGURE 3. ***In vitro* assessment of Ca^{2+}/CaM-regulated activity of IQ*lm* mutants of AC8 and $AC8_{\Delta 1-106}$.** Crude membranes prepared from HEK293 cells transiently transfected with 1 of 10 AC8 IQ*lm* mutants or 1 of 10 $AC8_{\Delta 1-106}$ IQ*lm* mutants were incubated with varying concentrations of Ca^{2+} in the presence of 1 μM CaM. Data sets, representative of at least three identical experiments, are presented as AC8 (*gray-filled circles*) and $AC8_{\Delta 1-106}$ (*open circles*) versions of the same IQ*lm* mutation, for comparison (*i–x*). Ca^{2+}-stimulated activities are expressed relative to basal activity in the absence of Ca^{2+}. The IQ*lm* sequence is displayed for reference and is *boxed* at the *top* of the figure. This sequence is reproduced at the head of every graph, where mutated residues are indicated in *underlined boldface type*.

imal leucine residues at the C-terminal end of the sequence was mutated (L1208/L9E). To our surprise, the *in vitro* Ca^{2+}/CaM stimulation of all of these mutants was robust, and neither the EC_{50} nor maximal relative activation values deviated significantly from WT-AC8 (Fig. 3, *i–x*). Even the mutant in which all consensus IQ*lm* residues were substituted by alanine, $AC8^{VQR/AAA}$, exhibited a Ca^{2+} stimulation profile akin to WT-AC8 (Fig. 3, *vi*). Fig. 4*A* presents the mean maximal stimulation by Ca^{2+}/CaM relative to basal for WT-AC8 and all mutants, as taken from at least three separate experiments. The variability was substantial, but stimulation by Ca^{2+}/CaM was consistent. One-way analysis of variance confirms that none of the IQ*lm* data sets deviate significantly from that of WT-AC8. When [Ca^{2+}] was kept constant and [CaM] changed to produce CaM concentration-effect curves for selected IQ*lm* mutants (supplemental Fig. 3), again little difference was observed between WT-AC8 and IQ*lm* mutant profiles.

The emergence of a Ca^{2+}-stimulable AC activity after transfection of AC8 clearly indicates expression of the construct, so that all AC8 IQ*lm* mutants must be efficiently expressed by virtue of their uncompromised Ca^{2+} stimulation. Evidently then, either the targeted residues are not involved in association with Ca^{2+}/CaM to any extent or the presence of the N terminus, with its 1-5-8-14 CaMBD, compensates for putative mutational consequence at the C terminus. We considered the latter proposal more credible because of the following. (i) The amino acids that define the sequence as a CaM-binding IQ-like motif would reasonably be expected to be involved in CaM association (34). (ii) Other studies have shown that single or double substitutions in CaMBDs can ablate CaM binding and Ca^{2+}/CaM-dependent processes (35–37). (iii) The provision by N-terminal tethering of an equimolar CaM/effector ratio might potentially compensate for moderate attenuation of binding efficiency at the C-terminal effector site if that CaM was accessible to the C terminus. Clearly then, an alternative strategy was required to functionally assess the IQ*lm* in detail. Consequently, galvanized by the assurance that $AC8_{\Delta1-106}$ replicates a WT-like profile in the *in vitro* assays (Fig. 2), we introduced an identical set of IQ*lm* mutations into parent $AC8_{\Delta1-106}$ so that any contribution from the N-terminal CaMBD could be avoided.

Removal of the N-terminal 106 Residues of AC8 Uncovers Consequences of IQlm Mutations—Representative $AC8_{\Delta1-106}$ mutant data sets are shown alongside their AC8 counterparts for comparison (Fig. 3, *i–x*). Several of the $AC8_{\Delta1-106}$ IQ*lm* mutants displayed attenuated mean maximal stimulation by Ca^{2+}/CaM. When representative $AC8^{VN}$ and $AC8_{\Delta1-106}{}^{VN}$ data sets are juxtaposed (Fig. 3*i*), it is clear that a lower Ca^{2+}/CaM stimulation is observed in the absence of the N terminus. The mean maximal Ca^{2+}/CaM-induced activity of $AC8^{VN}$ was 4.3-fold, whereas that of $AC8_{\Delta1-106}{}^{VN}$ was 2.3-fold ($p < 0.05$, unpaired *t* test; Fig. 4, *A* and *B*). $AC8_{\Delta1-106}{}^{VN}$ also differed significantly from parental $AC8_{\Delta1-106}$ ($p < 0.01$; Fig. 4*B*). There seemed to be a slight difference in Ca^{2+}/CaM regulation between $AC8^{RQ}$ and $AC8_{\Delta1-106}{}^{RQ}$, from the representative Ca^{2+} concentration-effect curves (CECs) in Fig. 3*ii*; although across three identical assays, maximal activities were 4.1- and 3.3-fold, respectively, this difference did not reach significance ($p > 0.05$). $AC8_{\Delta1-106}{}^{RQ}$ activity was lower than parental $AC8_{\Delta1-106}$ ($p < 0.01$; Fig. 4*B*). When both V1197N and R1202Q were combined to produce $AC8^{VR/NQ}$ and $AC8_{\Delta1-106}{}^{VR/NQ}$, the activity of the former was not affected (Fig. 4*A*), but the activity of the latter was severely compromised at a mere 1.2-fold (Fig. 4*B*). Representative CECs illustrate this discrepancy (Fig. 3*iii*). The single point mutation Q1198K did not alter the Ca^{2+}/CaM regulation of AC8 or $AC8_{\Delta1-106}$ because both $AC8^{QK}$ and $AC8_{\Delta1-106}{}^{QK}$ displayed robust activation (6.4 ± 2.1 and 5.3 ± 0.5, respectively), which was equivalent to parental AC8 and $AC8_{\Delta1-106}$ (Fig. 3*iv* and Fig. 4*B*). Therefore, V1197N was the most detrimental single point mutation to $AC8_{\Delta1-106}$ activity, with R1202Q also reducing Ca^{2+}/CaM regulation, albeit to a lesser extent. Q1198K did not compromise the activity of either AC8 or $AC8_{\Delta1-106}$. Combining V1197N and R1202Q mutations resulted in a near-ablated Ca^{2+}/CaM response of $AC8_{\Delta1-106}$, but not of AC8, which remained robust.

The double and triple alanine substitution mutants, $AC8_{\Delta1-106}{}^{VQ/AA}$ and $AC8_{\Delta1-106}{}^{VQR/AAA}$ both displayed significantly attenuated maximal stimulation by Ca^{2+}/CaM (Fig. 3, *v* and *vi*). Over three similar experiments both diverged from parental $AC8_{\Delta1-106}$ by one-way ANOVA (Fig. 4*B*). Additionally, *t* tests revealed these data differed statistically from the corresponding AC8 mutants ($p < 0.05$ for $AC8^{VQ/AA}$ *versus* $AC8_{\Delta1-106}{}^{VQ/AA}$ as well as for $AC8^{VQR/AAA}$ *versus* $AC8_{\Delta1-106}{}^{VQR/AAA}$). To confirm that the depressed activity of $AC8_{\Delta1-106}$ mutants was not because of potential effects on enzyme catalysis or expression level, stimulation by the generic AC activator FSK was assessed *in vitro*, and Western blots were performed using membrane samples (supplemental Figs. 4 and 5, respectively). Expression was confirmed for all $AC8_{\Delta1-106}$ IQ*lm* mutants. $AC8_{\Delta1-106}{}^{VQ/AA}$ and $AC8_{\Delta1-106}{}^{VQR/AAA}$ were activated by FSK to a level far greater than their modest Ca^{2+} responses and similar to their AC8 counterparts, arguing against any effect on general enzyme function. Taken together, these data suggest that mutation of Val^{1197} and Gln^{1198} significantly attenuates but does not ablate Ca^{2+}/CaM regulation of AC8, whereas the additional Arg^{1202} mutation exacerbates this reduction, so that little stimulation by Ca^{2+}/CaM survives.

Three positively charged amino acid side chains are present in the AC8 IQ*lm*, provided by two arginines and one lysine regularly spaced in the middle of the motif. Two mutations, R1202/4E and K1206E, sought to assess the reliance of AC8 activation on these charged features by substitution with glutamate, an amino acid of opposing polarity. As with all other AC8-based mutations, both $AC8^{RR/EE}$ and $AC8^{KE}$ were strongly stimulated by Ca^{2+} in the presence of exogenous CaM (8.7- and 5.0-fold, respectively). Representative CECs indicate that the maximum Ca^{2+}/CaM activity of $AC8_{\Delta1-106}{}^{KE}$ was lower than $AC8^{KE}$, and the EC_{50} value for Ca^{2+} was increased. Over three similar experiments, the mean maximal Ca^{2+} stimulation of $AC8_{\Delta1-106}{}^{KE}$ (2.7-fold) was lower than that of $AC8^{KE}$ (5.0-fold); the difference between data sets was quantified by a *p* value of < 0.05 (Fig. 4). Possible concerns with expression and catalytic fidelity can again be put aside given the strong FSK stimulation of $AC8_{\Delta1-106}{}^{KE}$ (supplemental Fig. 4). However, the Ca^{2+} activation of $AC8_{\Delta1-106}{}^{RR/EE}$ was nearly ablated,

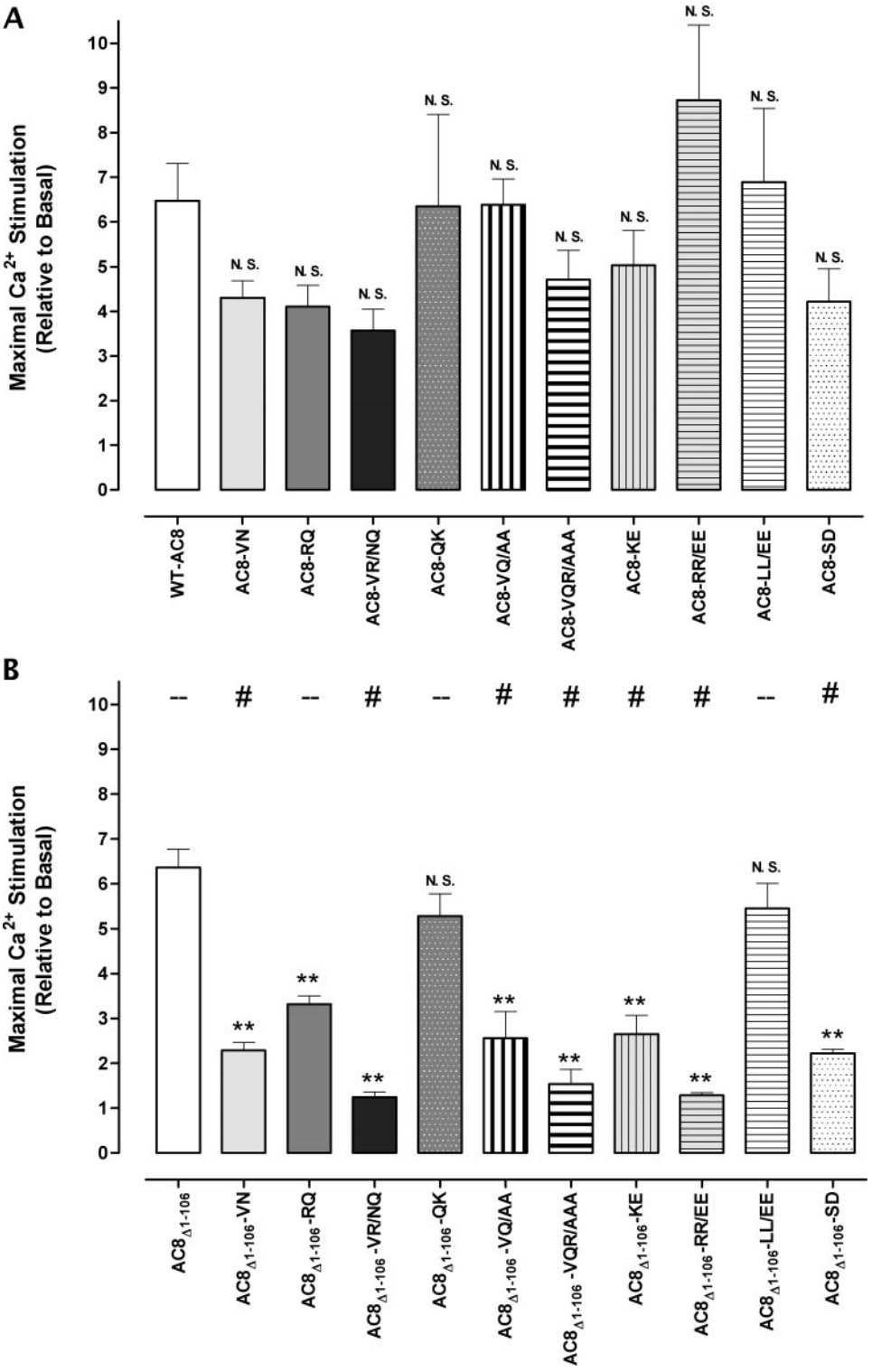

FIGURE 4. **Mean maximal Ca^{2+}/CaM-regulated activity of AC8 and $AC8_{\Delta 1-106}$ IQ*lm* residue mutants.** Maximal Ca^{2+} stimulations, expressed relative to basal activity, in the presence of 1 μM CaM are shown as the mean ± S.E. for all AC8 IQ*lm* mutants collectively (*A*) and all $AC8_{\Delta 1-106}$ mutants collectively (*B*). Within these two data sets, Dunnett's multiple comparison tests were employed, where *N.S.* denotes no significant change from parental AC8/$AC8_{\Delta 1-106}$, and ** denotes a difference with an associated $p < 0.01$. Data are arranged such the $AC8_{\Delta 1-106}$ version of an IQ*lm* is shown directly *below* the AC8 version. Unpaired *t* tests were conducted between horizontally aligned $AC8_{\Delta 1-106}$ and AC8 IQ*lm* mutant data sets for each mutant, where − represents $p > 0.05$ (not significant) and # represents $p < 0.05$.

yielding a mere 1.3-fold stimulation over basal activity (Fig. 3*viii* and Fig. 4*B*). This AC was expressed efficiently, and its FSK-induced activity was robust (supplemental Fig. 4 and Fig. 5*C*), indicating that the mutation produced a discrete reduction of Ca^{2+}/CaM stimulation.

The presence of amino acids with large, hydrophobic side-chains typifies CaM-binding sequences (4). The exposure of nonpolar grooves in both CaM lobes after Ca^{2+} binding provides essential loci for interaction with hydrophobic amino acids of target sequences. Accordingly, and aside from a valine residue already discussed above, the AC8 IQ*lm* contains four leucine residues as follows: two are adjacent and sequentially more C-terminal, and the another two are close to each other but sequentially more N-terminal. The C-terminal Leu^{1208} and Leu^{1209} were substituted by glutamate. $AC8^{LL/EE}$ and $AC8_{\Delta 1-106}{}^{LL/EE}$ had similar levels of stimulation by Ca^{2+}/CaM (6.9- and 5.5-fold, respectively; Fig. 3*ix* and Fig. 4, *A* and *B*), indicating that, because this mutation was well tolerated, these C-terminal hydrophobic residues do not play an important part in stimulation of AC8.

The S1199D mutation aimed to initiate a consideration of local phosphorylation at the only candidate residue of the sequence. The negatively charged side chain of aspartate approximates the presence of a phosphate group added to serine. Although the IQ*lm* sequence does not provide this serine with the characteristic basic residue at the −3 position, it does lend hydrophobic residues at −5 and +1, which have been found to be important for CaMKII and CaMKIV recognition (38). As with all other IQ*lm* mutants introduced to the whole AC8 enzyme, little effect was observed with the introduction of S1199D; stimulation by Ca^{2+}/CaM was robust at 4.2-fold and not significantly different from that of WT-AC8 (Fig. 4*A*). In the absence of the N terminus, however, maximal Ca^{2+}/CaM stimulated activity was stunted at 2.2-fold (Fig. 4*B*). The difference between $AC8^{SD}$ and $AC8_{\Delta 1-106}{}^{SD}$ is clear from the representative CECs depicted in Fig. 3*x*.

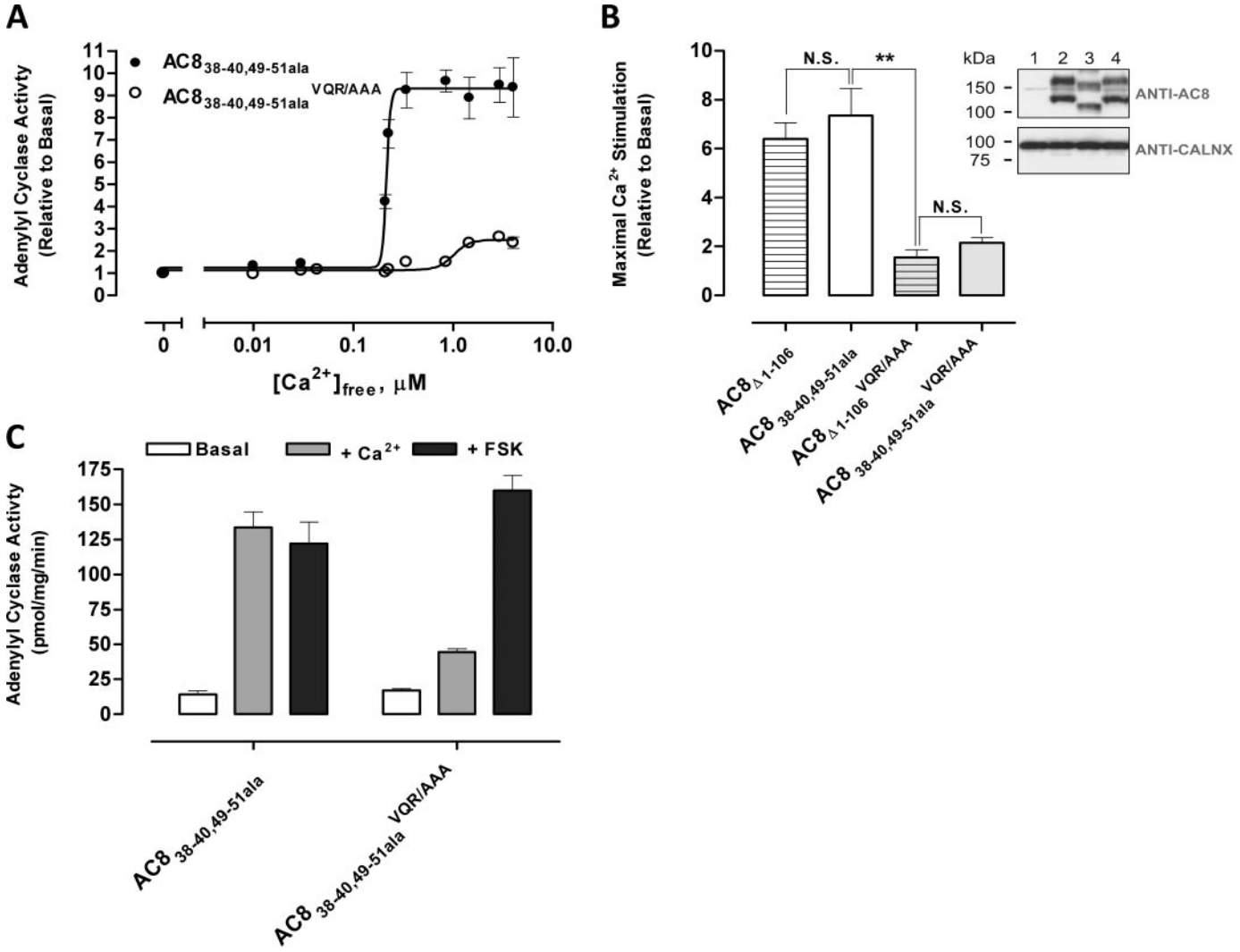

FIGURE 5. **N-terminal CaM-binding mutant $AC8_{38-40,49-51ala}$ reproduces $AC8_{\Delta1-106}$ activity *in vitro*, and IQ*lm* mutants of both have similarly attenuated Ca^{2+}/CaM regulation.** *A*, crude membranes prepared from HEK293 cells transiently transfected with $AC8_{38-40,49-51ala}$ show robust stimulation by Ca^{2+} in the presence of 1 μM CaM (EC_{50} = 0.21 μM), but those transfected with $AC8_{38-40,49-51ala}^{VQR/AAA}$ exhibit an attenuated Ca^{2+}/CaM activity with a reduced affinity for Ca^{2+} (EC_{50} = 1.01 μM). *B*, over three experiments, the relative maximal stimulation by Ca^{2+}/CaM of $AC8_{38-40,49-51ala}$, $AC8_{38-40,49-51ala}^{VQR/AAA}$, $AC8_{\Delta1-106}$, and $AC8_{\Delta1-106}^{VQR/AAA}$ were compared using one-way ANOVA with Newman-Kuels multiple comparison test (data shown are mean ± S.E.). *N.S.*, not significant. *C*, $AC8_{38-40,49-51ala}$ displays robust Ca^{2+}/CaM stimulation that approaches that elicited by 10 μM FSK, whereas the Ca^{2+}/CaM activation of $AC8_{38-40,49-51ala}^{VQR/AAA}$ was significantly reduced, although FSK-induced activity was unimpaired. *Inset*, Western blotting (*lane 1*, untransfected control; *lane 2*, $AC8_{38-40,49-51ala}$; *lane 3*, $AC8_{\Delta1-106}^{VQR/AAA}$; *lane 4*, $AC8_{38-40,49-51ala}^{VQR/AAA}$) confirmed expression of $AC8_{38-40,49-51ala}^{VQR/AAA}$. Membrane samples were probed using AC8 (anti-AC8) and calnexin (anti-CLNX) antibodies. Calnexin immunodetection was included as a loading control.

Only the CaM-binding Domain Residues in the N Terminus Confer Insensitivity of the Full-length AC8 to IQlm Mutations—The consequences of the IQ*lm* residue mutations detailed above were only manifest when the N-terminal truncation mutant $AC8_{\Delta1-106}$ was used as the parent molecule for mutagenesis. This use of $AC8_{\Delta1-106}$ was validated by the established observation that in the *in vitro* context, $AC8_{\Delta1-106}$ is indistinguishable from AC8 in the presence of exogenous CaM. The 1-5-8-14 motif lies between amino acids 34 and 52, so 88 non-CaMBD residues are deleted in $AC8_{\Delta1-106}$. Therefore, we asked whether uncovering the consequences of the C-terminal IQ*lm* mutations was due simply to the lack of CaM binding or to some other structural effect, resulting from removal of the N terminus. Another previously characterized mutant (11) (originally named M34 but hereafter referred to as $AC8_{38-40,49-51ala}$) was ideal for this purpose because six alanine substitutions imposed at key positions of the 1-5-8-14 motif render it impotent at binding CaM at the N terminus (39). Taking an effective IQ*lm* mutation as an example, we introduced the consensus residue triple substitution to the C terminus of $AC8_{38-40,49-51ala}$, thereby creating $AC8_{38-40,49-51ala}^{VQR/AAA}$. This latter mutant displayed a Ca^{2+}/CaM stimulation of only 2.15 ± 0.21-fold over basal as compared with 7.34 ± 1.12 with $AC8_{38-40,49-51ala}$ (Fig. 5*A*); a similar severity of attenuation in terms of maximal Ca^{2+} stimulation was between $AC8_{\Delta1-106}^{VQR/AAA}$ and $AC8_{\Delta1-106}$ (Fig. 5*B*). The comparable maximal Ca^{2+}/CaM stimulation (6.39 ± 0.56 and 7.34 ± 1.12, respectively) of the two N-terminal mutants used here, $AC8_{\Delta1-106}$ and $AC8_{38-40,49-51ala}$, validates their use as bases to explore mutations in the IQ*lm* motif. Fig. 5*B* (*inset*)

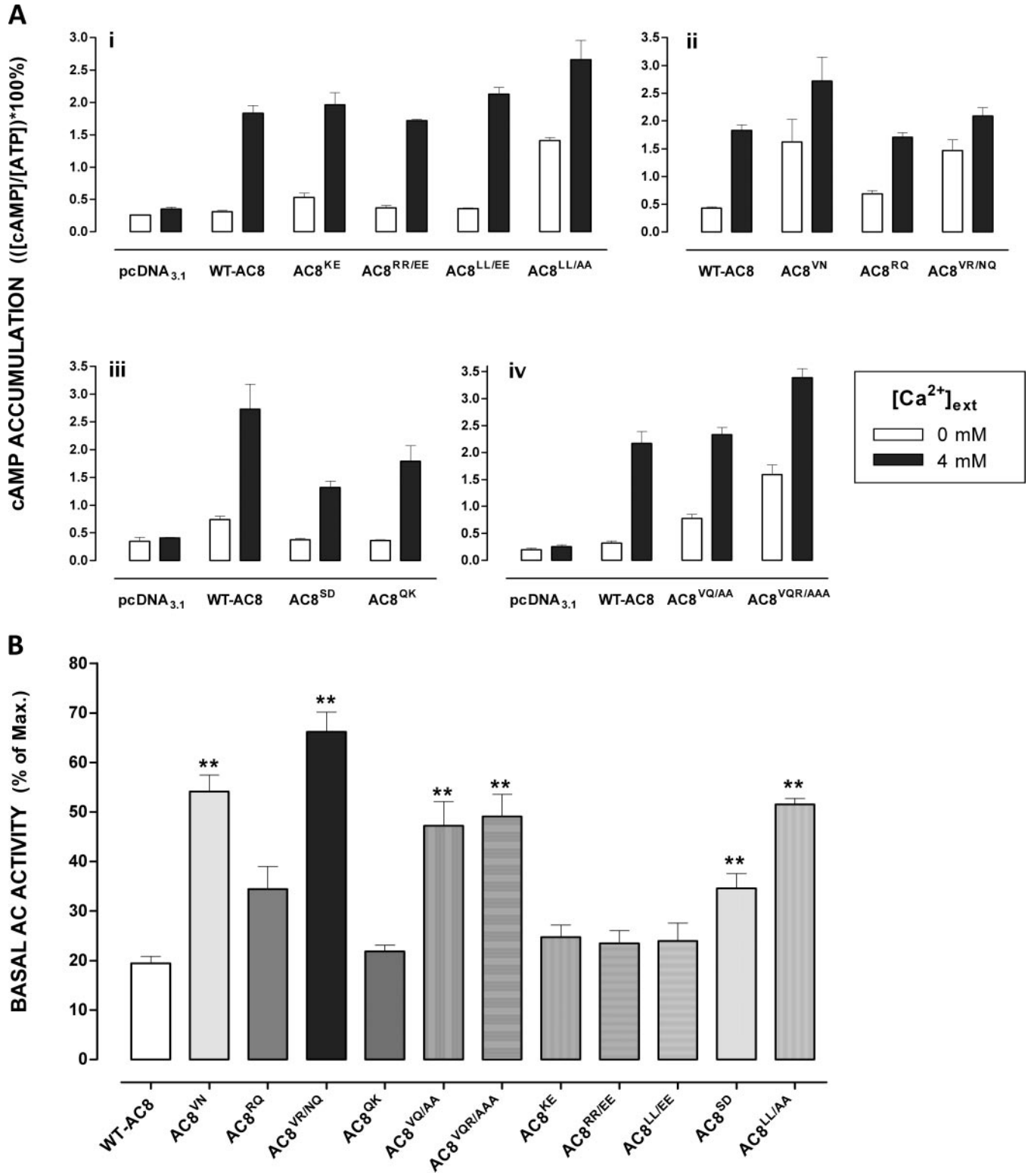

FIGURE 6. **Cell population studies reveal Ca^{2+}-independent activity of Val^{1197} and $Leu^{1196/1200}$ IQ*lm* mutants, associated with disinhibition.** *A*, representative cAMP accumulation assay sets from AC8 IQ*lm* mutants. 100 nM TG was used to empty intracellular Ca^{2+} stores 4 min prior to external addition of 0 mM Ca^{2+} (no CCE) or 1, 2, or 4 mM Ca^{2+} to evoke CCE of increasing magnitude (see supplemental Fig. 2*A* for the corresponding $[Ca^{2+}]_i$ rises). *B*, using data from three such assays, cAMP accumulation at 0 mM Ca^{2+} was expressed relative to the maximum Ca^{2+}-evoked accumulation at 4 mM, for WT-AC8, and each IQ*lm* mutant (mean ± S.E.). One-way ANOVA followed by Dunnett's multiple comparisons test indicated significant differences in normalized Ca^{2+}-independent activity of some mutants compared with WT-AC8 (where ** denotes $p < 0.01$).

indicated that $AC8_{\Delta 1-106}{}^{VQR/AAA}$ was robustly expressed and that the FSK stimulation of $AC8_{\Delta 1-106}{}^{VQR/AAA}$ was robust and far greater than the level seen with Ca^{2+}/CaM (Fig. 5*C*). We consequently concluded that it was simply the CaM binding property of the N-terminal region that compensated for mutations at the C-terminal IQ*lm*.

Selective Contribution of IQlm Amino Acids to Autoinhibition Is Observed in Intact Cells—Thus far, we had examined the IQ*lm* mutants in an *in vitro* assay system where [CaM] is readily controlled. We wished to address the significance of these mutations in the more realistic setting of the intact cell, where AC8 must compete with the plethora of other CaM-binding proteins for CaM, a situation that might be expected to exacerbate compromised CaM binding. Whole-cell cAMP accumulation assays were seen to be an appropriate means to test basal activity and thereby CaM-independent relief of autoinhibition (in addition to CCE-mediated Ca^{2+} stimulation; Fig. 1*D*). A limitation of this type of assay is that only AC8 species with intact N termini can be used. $AC8_{\Delta 1-106}$, for example, displays a greatly diminished response to Ca^{2+} entry by CCE, a deficit that is proposed to reflect the role of the N terminus in recruiting CaM (26) as well as possible association with other factors that confer sensitivity to CCE (11). Thus only full-length AC8 IQ*lm* mutants could be assessed. AC activity induced by CCE triggered by 4 mM Ca^{2+} in the extracellular medium was compared with the activity when Ca^{2+} was absent from the medium. Fig. 6*A, panels i–iv,* shows representative experiments for each of the mutants, and in Fig. 6*B* basal activity was expressed as a percentage of maximal Ca^{2+} activity over three identical assays. As in Fig. 1, very little Ca^{2+} stimulation is observed in pcDNA3-transfected cells, but a large (4–6-fold) enhancement is seen with high $[Ca^{2+}]_{ext}$ in AC8-expressing cells. Basal activity of WT-AC8 was routinely around 20% of the maximum Ca^{2+}-stimulated value. A similar relationship applies to $AC8^{KE}$, $AC8^{RR/EE}$, $AC8^{QK}$, and $AC8^{LL/EE}$ (Fig. 6, *A*, *panel i*, and *B*). Clearly, in this system these mutations were of little consequence to the CCE regulation of AC8. $AC8^{LL/AA}$ (in which Leu^{1196} and Leu^{1200} have been substituted with alanine), however, had a consistently high basal activity, with Ca^{2+} stimulation at a similar level to AC8. This elevated cAMP accumulation, manifest as 50% of maximum over three experiments, was more than 30% higher than wild type (Fig. 6*B*). Because an abnormally high constitutive activity indicates a relief of autoinhibition, Leu^{1196} and/or Leu^{1200} appear to contribute to the maintenance of the autoinhibited state. Considering $AC8^{VN}$, $AC8^{RQ}$, and $AC8^{VR/NQ}$ together, we see that the R1202Q mutation increased basal activity slightly (Fig. 6*A, panel ii*) but not significantly (Fig. 6*B*), and it still retained appreciable Ca^{2+} regulation. $AC8^{VN}$ and $AC8^{VR/NQ}$, however, both displayed significantly higher basal activity (Fig. 6, *A, panel ii,* and *B*); a minor contribution from Arg^{1202} is suggested from the more prominent basal activity of $AC8^{VR/NQ}$ compared with $AC8^{VN}$. So, it seemed that Val^{1197} played a privileged role in the stabilization of AC8 autoinhibition. This impression was further supported by two other mutants, $AC8^{VQ/AA}$ and $AC8^{VQR/AAA}$, both of which contained Val^{1197} substitutions, and displayed elevated basal activity (Fig. 6, *A, panel iv,* and *B*). The phosphomimetic S1199D mutation produced an enzyme whose maximal CCE regulation was consistently lower than WT-AC8 activity (Fig. 6*A, panel iii*). $AC8^{SD}$ also displayed a Ca^{2+}-independent activity that was significantly higher than that that of WT-AC8 (Fig. 6*B*). Thus Leu^{1196}, Leu^{1200}, Val^{1197}, and potentially Ser^{1199} are essential in maintaining the autoinhibited state.

Comparing the parallel display of *in vitro* basal, Ca^{2+}-, and FSK-stimulated activity for each of the AC8 IQ*lm* mutants (supplemental Fig. 4) allows some further insights. As shown in Fig. 1*C*, the maximal stimulation induced by Ca^{2+}/CaM equates with that achieved by FSK (seen again in supplemental Fig. 4*xi*). A number of the IQ*lm* mutants exhibited this same relationship, $AC8^{QK}$, $AC8^{RR/EE}$, $AC8^{KE}$, and $AC8^{LL/EE}$ (supplemental Fig. 4, *iv, vii, viii,* and *ix*, respectively). However, in the remainder of the AC8 mutants, the level of Ca^{2+} stimulation was substantially lower than that of FSK, *i.e.* $AC8^{VN}$, $AC8^{RQ}$, $AC8^{VR/NQ}$, $AC8^{VQ/AA}$, $AC8^{VQR/AAA}$, and $AC8^{SD}$ (supplemental Fig. 4, *i–iii, v, vi,* and *x*, respectively). This latter subset represents all the AC8 mutants that contain substitutions of the residues only proposed to contribute to autoinhibition.

Arg^{1202} and Arg^{1204} Are Essential for Efficient CaM Binding at the IQlm—The *in vitro* and whole-cell AC activity assays described above revealed a distinction between mutations of AC8 that affect Ca^{2+}/CaM stimulation and those that basally disinhibit activity. Therefore, we next wished to assess directly the CaM binding ability of IQ*lm* mutated sequences, which would distinguish the contribution of CaM binding from consequences for activity. To permit this analysis, the C2b region containing the IQ*lm* (Leu^{1183}–Pro^{1248}) was N-terminally fused to glutathione *S*-transferase (GST-8C2b), and the cDNA encoding this fusion was subject to the same site-directed mutagenesis used for the generation of AC8 and $AC8_{\Delta 1-106}$ mutants (supplemental Table 1) to create six example mutations of $GST\text{-}AC8_{C2b}$. A simple *in vitro* co-pulldown assay was then developed, which proved suitable to detect CaM binding by GST-8C2b (see "Experimental Procedures"). Our AC8 antibody recognizes an epitope at the extreme C terminus and thus can be used to confirm expression of the fusion proteins. GST alone did not bind CaM at any of the concentrations used, despite its presence at higher quantities than the fusion proteins (Fig. 7, *A–C*). However, GST-8C2b clearly bound CaM in a concentration-dependent manner. By contrast, the R1202E/R1204E mutant of GST-8C2b showed greatly diminished CaM binding, with only a faint signal at the maximal (1 μM) CaM input (Fig. 7*A*). By comparison, $GST\text{-}8C2b^{VQ/AA}$ appeared to bind CaM as strongly as the wild-type sequence. This latter observation is important as it implies that two of three consensus residues that define the sequence as a CaMBD are not directly involved in AC8 association with CaM at the C terminus. $GST\text{-}AC8_{C2b}{}^{LL/EE}$ pulled down equivalent levels of CaM to GST-8C2b at each concentration used, indicating that these mutations do not perturb CaM binding (Fig. 7*B*). The triple consensus residue mutant, $GST\text{-}8C2b^{VQR/AAA}$, could bind CaM, albeit to a lesser extent than the wild-type GST fusion construct. $GST\text{-}8C2b^{KE}$ and $GST\text{-}8C2b^{LL/AA}$ both displayed robust pulldown of CaM, indicating that neither mutation impedes CaM binding by the IQ*lm* (Fig. 7*C*).

The N and C Termini of AC8 Interact in a Manner That Is Abrogated by Ca^{2+}/CaM—A model of AC8 activation proposed in Ref. 26 suggests a proximity of the N and C termini of AC8, which allows the transfer of a CaM molecule from the N to the C terminus as the first stage in activation. However, direct evidence for association of these key regions of AC8 is not yet available. We hence asked whether these domains might

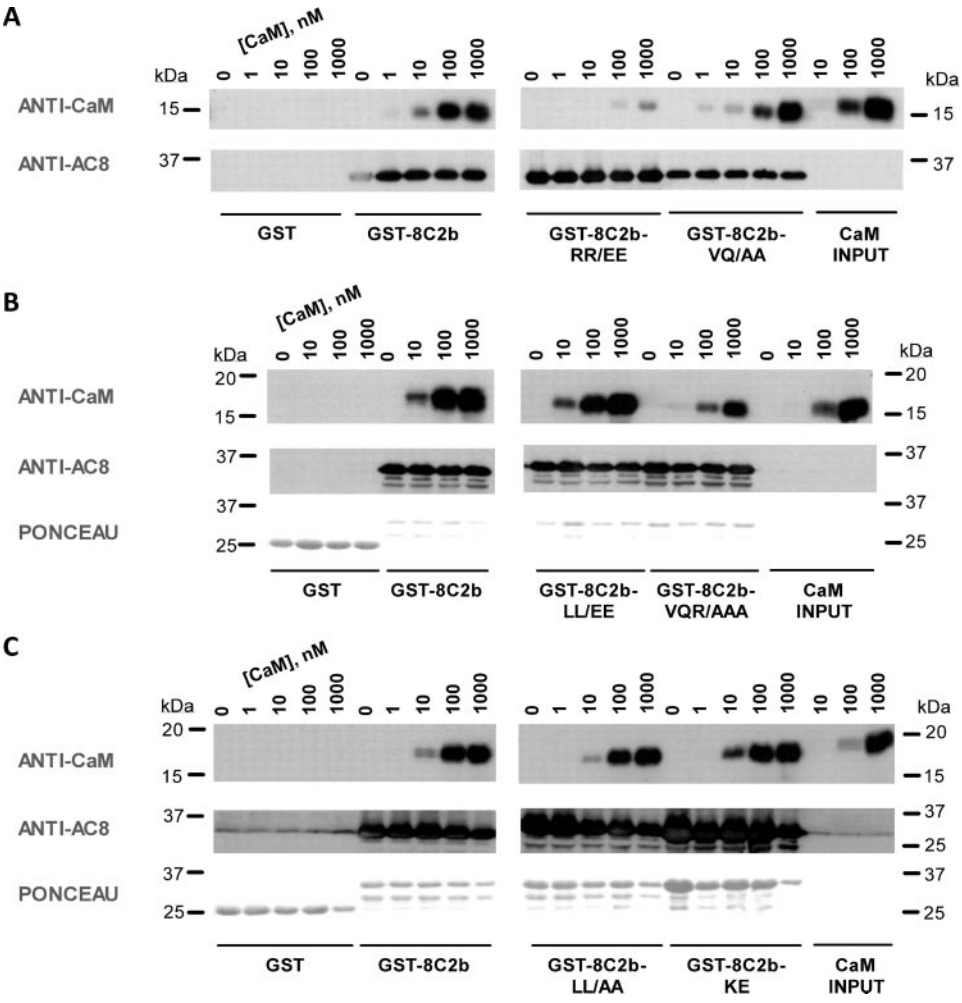

FIGURE 7. **Direct CaM binding of wild-type and mutant AC8 C2b regions indicates Arg^{1202} and Arg^{1204} as essential residues.** The C2b region of AC8-(1183–1248) was N-terminally fused to GST. The IQ*lm* therein was mutated in the same way as for the full-length AC8 and AC8$_{\Delta 1-106}$ used in functional assays (see "Experimental Procedures"). GST, GST-8C2b, and mutated GST-8C2b were purified and immobilized on glutathione-Sepharose resin. A simple pulldown assay established the level of binding to varying concentrations of CaM after 2 h at 4 °C (*anti-CaM rows*). CaM concentrations used in each column are indicated by vertical numbers (*nM CaM*). The wild-type and mutated GST-8C2b fusions all contain the epitope for the anti-AC8 antibody, so this was used to confirm input levels (*anti-AC8 rows*). Additionally, GST and GST fusion input was established with Ponceau staining (*Ponceau rows*).

associate in the presence and absence of Ca^{2+} and CaM. We generated an N-terminally maltose-binding protein (MBP)-tagged AC8 N terminus (MBP-8Nt) expressed in BL21 bacterial cells to facilitate this analysis. The soluble fraction from these cells was used as input in GST co-pulldown assays with GST-8Ct. In this experiment, GST or GST fusion proteins were used, immobilized on glutathione-Sepharose resin, as bait for MBP-8Nt. We also wanted to assess the effect of Ca^{2+}-saturated and Ca^{2+}-free CaM on any interaction observed. The overall assay design is depicted in Fig. 8*A*.

As presented in Fig. 8*B*, some pulldown of MBP-8Nt occurred with GST alone (*lane 1* of *GST* set), but substantially more signal is seen when immobilized GST-8Ct was used as bait (*lane 1* of *GST-8Ct*). This is quantified as 30% of the signal obtained with 1% MBP-8Nt input for GST, but the much higher 120% for GST-8Ct (Fig. 8*C*). However, when CaM was added to the mixture, less MBP-8Nt was pulled down by GST-8Ct (Fig. 8*B,* compare *lanes 1* and *2* under *GST-8Ct*) in the presence of Ca^{2+} (from 120% of input to 20%; see Fig. 8*C*). This coincided with a strong pulldown of CaM. In the presence of EGTA and CaM, however, only a very small amount of CaM is pulled down with GST-8Ct, and the level of associated MBP-8Nt partially recovers (to 60% of input, Fig. 8*C*). Less MBP-8Nt is pulled down in the presence of EGTA/CaM (*lane 3*) compared with EGTA only (Fig. 8*C, lane 1*), but this can be accounted for by the association of the AC8 N terminus with CaM in the absence of Ca^{2+} (26). Thus, MBP-8Nt and GST-8Ct could interact, but the binding of MBP-8Nt by GST-8Ct was specifically inhibited by Ca^{2+}/CaM rather than Ca^{2+}-free CaM. This indicates that the terminal domains of AC8 could interact at resting [Ca^{2+}], but this association was not supported when fully Ca^{2+}-saturated CaM is present. So, we envisage that, as developed under "Discussion," upon activation of AC8 by Ca^{2+}/CaM, its termini dissociate as part of the structural rearrangement responsible for relief of autoinhibition.

Given the above suggestion that terminal regions of AC8 interact as part of a resting autoinhibitory interaction, and a subset of IQ*lm* residues contributes to autoinhibition, we considered that Leu^{1196}, Val^{1197}, and Leu^{1200} might impart binding to the N terminus. So the GST-8C2b fusion protein, and mutants thereof, used in CaM binding assays were directly assessed for their ability to pull down MBP-8Nt (supplemental Fig. 7) in the same manner as described for GST-8Ct in the absence of Ca^{2+}/CaM. GST-8C2b is shorter than GST-8Ct, but it could associate effectively with MBP-8Nt, as shown by the greatly increased signal observed relative to GST alone (supplemental Fig. 7*A*). When the level of MBP-8Nt is expressed as a function of the total input signal of the GST or GST fusion lanes (including degradation products of the latter), GST-8C2b pulled down 2.3-fold more MBP-8Nt than GST alone. By the same analysis, the inherent mutations in GST-8C2b-VQ/AA reduced this binding efficiency to 1.7-fold over basal. The association of GST-8C2b-LL/AA with MBP-8Nt was equivalent to the nonspecific binding seen with GST, which indicated that the L1196A/L1200A double substitution abolished specific binding of the two termini of AC8. Therefore, it seems from this experiment that Leu^{1196} and Leu^{1200} are major determinants of autoinhibition by pro-

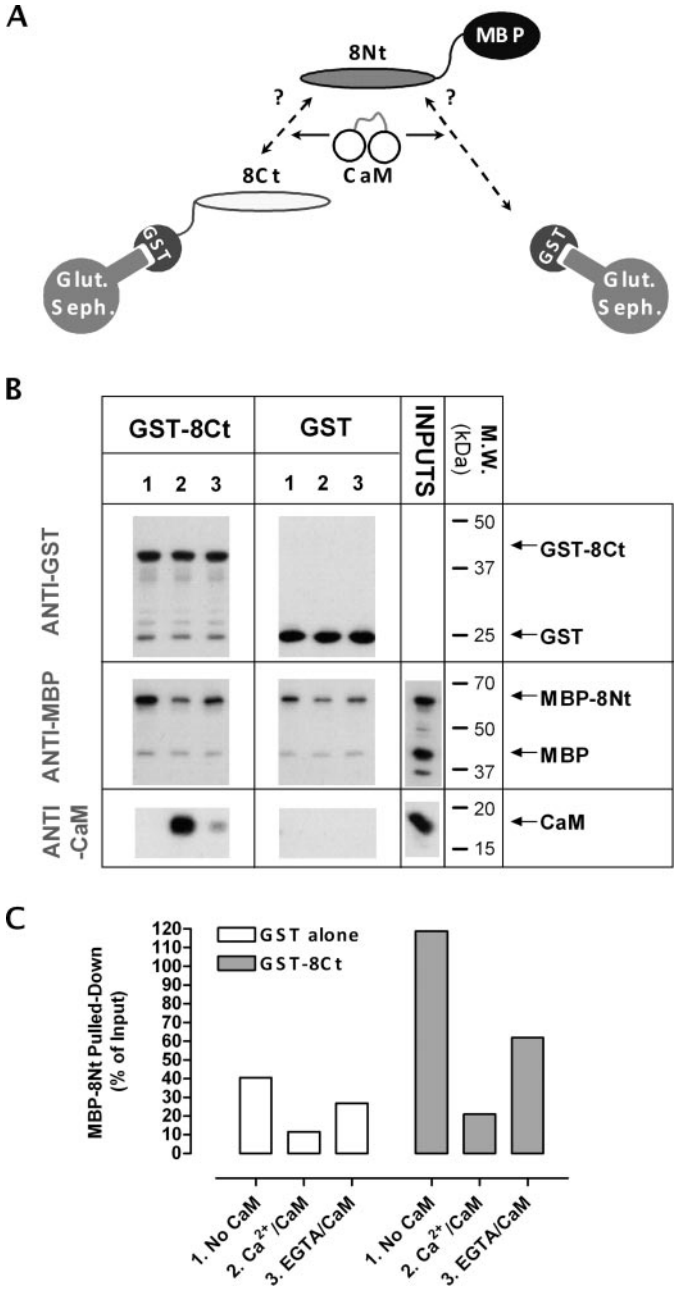

FIGURE 8. **Ca^{2+}/CaM selectively inhibits the interaction of differentially tagged AC8 N and C termini.** *A*, pictorial representation of a pulldown assay designed to assess interaction of the N and C termini of AC8. GST-tagged AC8 C terminus (GST-8Ct) was used as bait for MBP-tagged AC8 N terminus (MBP-8Nt), and the effect of Ca^{2+}-free and separately Ca^{2+}-saturated CaM on the interaction was tested. *B*, shown are Western blots from pulldown assays MBP-8Nt from bacterial lysates using glutathione-Sepharose complexed with GST or GST-8Ct. *Vertical text* on the *left side* indicates the antibody used. Three conditions were analyzed as follows: *lane 1*, 200 μM EGTA, no CaM; *lane 2*, 20 μM Ca^{2+} and 1 μM CaM; *lane 3* 200 μM EGTA and 1 μM CaM. *Input lanes* indicate 1% input levels of CaM and bacterial lysate containing MBP-8Nt. *C*, signal intensities were quantified using ImageJ software (National Institutes of Health), and the level of MBP-8Nt pulled down in each test lane is expressed as a percentage of the signal intensity of the uppermost MBP-8Nt input band (which represents the intact fusion protein).

moting interaction of the N and C termini of AC8. Although Val^{1197} likely contributes to this same process, its importance is less emphatic, indicating that other regions of AC8, in the native domain organization, also play a role in maintaining the autoinhibited state.

DISCUSSION

The regulation by Ca^{2+} of ion channels and signaling enzymes can be expected to be sophisticated, given the importance of this mode of influencing cellular activity. Nevertheless, the expanding range of modes of utilization of this device continues to be surprising. In particular, CaM regulatory formats are emerging as mechanistically highly diverse (40). In this regard, some processes such as complex Ca^{2+}-dependent facilitation or inactivation of various voltage-gated Ca^{2+} channels (41) are becoming well understood, and yet the activation of an apparently simple enzyme, AC8, by Ca^{2+}/CaM turns out to involve unexpected layers of complexity. Initial studies identified a CaM-binding domain at each terminus of AC8, but only one was required for stimulation of catalytic activity, in an apparently disinhibitory mechanism (24). A later study suggested a role in the intact cell for the catalytically less significant N-terminal binding domain (11), and most recently this domain was viewed to provide a stable reserve of CaM for use by the C terminus (26). In this study we tried to unravel and reconcile these interactions by a series of *in vitro* and intact cell experiments on variously mutated and truncated AC8 constructs.

A series of deletion mutants first revealed that the CaMBD and autoinhibitory domain of AC8 co-localized to the region between Val^{1197} and Leu^{1212}. Truncation from 1212 to 1248 did not affect AC8 activity as measured *in vitro* or in cell population cAMP accumulation assays. Only when the majority of the IQ*lm* was deleted did the resulting enzyme become almost unresponsive to Ca^{2+} stimulation. The observation that a little Ca^{2+}/CaM-dependent activity persisted after this deletion agrees with the finding that an even more severe truncation of the entire C2b region, Δ1184–1248, retained some stimulability (24). This finding was recapitulated in the present series of experiments (supplemental Fig. 2*B*) and might be taken to suggest some interaction between CaM bound at the N terminus and the catalytic domains. Only AC8Δ4 (truncated from Val^{1197}) displayed robust disinhibited activity in the absence of Ca^{2+} in cell population assays. AC8Δ1, AC8Δ2, and AC8Δ3 all resembled WT-AC8 with regard to Ca^{2+}/CaM stimulation *in vitro* and in cell populations. Thus, we considered that the IQ*lm* contains both autoinhibitory and CaM-binding elements, which could either be overlapping (like those found in skeletal myosin light chain kinase, plasma membrane Ca^{2+}-ATPase, and CaM-dependent kinase II (42)) or spatially distinct, even within this short sequence.

In attempting to separate these two functions of the IQ*lm*, a number of point mutations (single and multiple) were introduced in this domain. To our considerable surprise, although the maximal Ca^{2+}/CaM stimulation varied somewhat between preparations, all mutants displayed a robust Ca^{2+}/CaM stimulation *in vitro* that was basically indistinguishable from that of WT-AC8. We speculated that pre-associated CaM at the N terminus could allow Ca^{2+}/CaM activation to proceed even in the presence of mutation at the C-terminal IQ*lm*. This speculation was consolidated when we introduced the same IQ*lm* mutations into $AC8_{\Delta 1-106}$, a truncation that lacks the N-terminal CaMBD. Two IQ*lm* mutations, L1208E/L1209E and

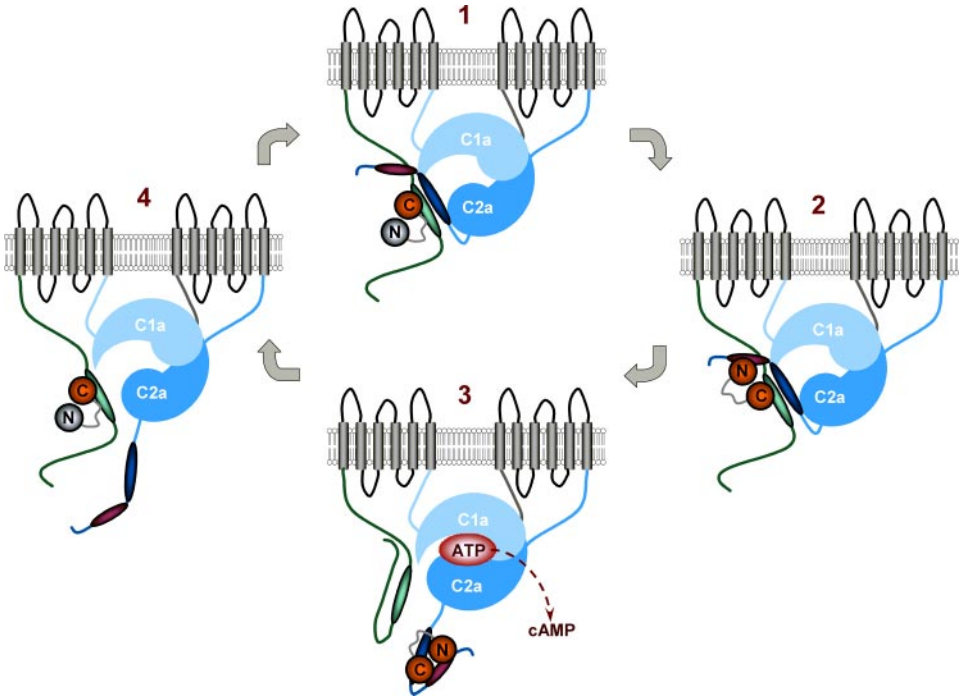

FIGURE 9. **Proposed mechanism of AC8 activation by CaM.** The dumb-bell represents CaM, where *N* and *C* indicate N- and C-lobes, respectively. *Orange* depicts Ca^{2+} saturation of a CaM lobe, and *gray* depicts a Ca^{2+}-free state. The 1-5-8-14 motif is represented by a *green ovoid*. The IQ*lm* is represented by two separate but connected *ovals*; *purple* denotes H1, and *blue* indicates H2. At rest (*stage 1*), the N and C termini of AC8 interact, as part of a larger autoinhibitory complex, with CaM pre-associated at the N-terminal 1-5-8-14 motif via its Ca^{2+}-saturated C-lobe. Upon a Ca^{2+} rise (*stage 2*), the N-lobe of CaM becomes Ca^{2+}-saturated (indicated by a change of color from *gray* to *orange*) and subsequently binds to H1 of the C-terminal IQ*lm*. Fully Ca^{2+}-saturated CaM then leaves the 1-5-8-14 motif (*stage 3*), binding solely to the IQ*lm*, and the whole autoinhibitory complex dissociates, resulting in activation of AC8. As local Ca^{2+} concentrations decrease, the N-lobe of CaM becomes Ca^{2+} free and binds once more to the 1-5-8-14 motif (*stage 4*), whereupon the whole system returns to rest with the re-association of the autoinhibitory complex (1).

Q1198K, were of no consequence to $AC8_{\Delta 1-106}$ activity, so we can propose that these residues are not involved in the activation of AC8. However, all other mutations inhibited the maximal Ca^{2+} stimulation of $AC8_{\Delta 1-106}$, in the following rank order: R1202E/R4E = V1197N/R1202Q > V1197A/Q1198A/R1202A > S1199D > V1197N > V1197A/Q1198A > K1206E > R1202Q. So not only does CaM tethering advantageously sequester a limited cellular transduction factor, it also might support the CaM-regulated activity of AC8. The latter must be a minor effect because the N-terminal truncation mutant, $AC8_{\Delta 1-106}$, retains full Ca^{2+}-dependent stimulation *in vitro*. To confirm that the deleted 106 amino acids performed no other function in this context than binding CaM, we introduced the V1197A/Q1198A/R1202A triple substitution into an AC8 mutant that retains the N terminus but is mutated in six critical residues in the CaMBD ($AC8_{38-40,49-51ala}$), so that it can no longer bind CaM (39). $AC8_{38-40,49-51ala}$ is functionally equivalent to $AC8_{\Delta 1-106}$ *in vitro*, because Ca^{2+}/CaM stimulation is not affected, but it is dependent on exogenous CaM for activity (26). $AC8_{38-40,49-51ala}{}^{VQR/AAA}$ displayed a similar degree of attenuation in Ca^{2+}/CaM activity as did $AC8_{\Delta 1-106}{}^{VQR/AAA}$, when compared with the respective parent mutant enzymes. This emphatically suggests that the CaM-binding residues of the N-terminal 1-5-8-14 motif, and not any others contained in the first 106 amino acids, impart tolerance to mutation of the IQ*lm*.

Intact cell assays assessed the cellular consequences on the disruptions caused by AC8 IQ*lm* mutations. Again, overall levels of Ca^{2+} stimulation seemed unaffected for all mutations (as with AC8 mutations *in vitro*), but, very strikingly, the Ca^{2+}-independent activity of those containing Val^{1197} and $Leu^{1196/1200}$ substitutions were significantly higher than WT-AC8. This Ca^{2+}-independent activity reflects disinhibition, so that the contribution of Val^{1197} and $Leu^{1196/1200}$ to the maintenance of an autoinhibited state is promoted.

Direct CaM binding of GST-fused C2b regions allowed us to separate binding from the functional effects of IQ*lm* mutants. This revealed that the mutation R1202E/R1204E almost ablated association of the C2b region with CaM, whereas V1197A/Q1198A, L1196S/L1200A, and L1208E/L9E were of little consequence. Hence, two of the three signature IQ-like residues are not directly involved in CaM binding, but the third plus another noncanonical more C-terminal arginine are critical. The diminished regulation by Ca^{2+}/CaM of $AC8_{\Delta 1-106}{}^{VQ/AA}$, $AC8_{\Delta 1-106}{}^{VQR/AAA}$, and $AC8_{\Delta 1-106}{}^{VN}$ *in vitro* is most probably because of an inherently elevated basal production of cAMP, which limits further activation by Ca^{2+}/CaM. The key residues of autoinhibition appear then to be Leu^{1196}, Val^{1197}, and Leu^{1200}, which do not contribute directly to Ca^{2+}/CaM binding.

Very little is known about the precise organization of the cytosolic regions of AC8, other than the certainty that catalytic C1a and C2a domains dimerize to form the catalytic core (43). Here we have shown that a GST-tagged C terminus interacts with an MBP-tagged N terminus and that this association is abrogated by Ca^{2+}-loaded, but not Ca^{2+}-free, CaM. It is further suggested that Leu^{1196} and Leu^{1200} are key to the interaction of the C2b region and N terminus, with a lesser contribution from Val^{1197}. This experiment reinforces our cell population cAMP assays that showed the importance of these residues in autoinhibition. We also now entertain the possibility that, although having a minor role in inter-termini association, Val^{1197} acts as an autoinhibitory anchor to distinct regions of AC8. This could involve either one or both of the catalytic C1a/C2a domains.

On the basis of the current experiments and previous work, we would now propose a new model for the regulation of AC8 by Ca^{2+}/CaM and the steps involved. We propose that CaM pre-associated at the N terminus of AC8 is incorporated into an autoinhibitory complex, involving the C terminus, at resting Ca^{2+} levels. From previous work, we suggest that Ca^{2+} binds to

the C-lobe of CaM (26), which has the higher affinity for [Ca^{2+}] than the N-lobe, an affinity that is potentially enhanced by association with the 1-5-8-14 sequence. The IQ*lm* of AC8, like many other CaM-binding sequences, is predicted to be α-helical in structure. Using Jpred, an on-line server that provides predictions from six secondary structure algorithms (44, we find a break in the helix at residue Asn^{1201} (supplemental Fig. 6). This break bifurcates the following two groups of amino acids we have now characterized: those that contribute mostly to basal autoinhibition (Leu^{1196}, Val^{1197}, and Leu^{1200}), and those that are directly involved in CaM binding (Arg^{1202} and Arg^{1204}). Perhaps this proposed break in structure reflects a separation of function of IQ*lm* residues. If the helical region before the break is called H1 and the helical region after the break is called H2, it is seen that H1 is highly hydrophobic and H2 contains all of the positively charged residues of the entire IQ*lm* (supplemental Fig. 6). These features may be important for the divergent responsibilities we propose for the residues therein. Incorporating this into the data described above, it is conceivable that H1 is buried in the autoinhibitory complex, and H2 is solvent-exposed, because of their respective nonpolar and polar characters. Therefore, we present a resting organization schematized in *state 1* of Fig. 9. A previous study concluded that CaM pre-associates with the 1-5-8-14 motif via its C-lobe, and here we have demonstrated a resting interaction of the N and C termini. By this arrangement, H2 might act as a hook for a Ca^{2+}-loaded CaM N-lobe, bait which is only available after initiation of the Ca^{2+} signal when pre-associated CaM senses a rise in Ca^{2+} via its basally Ca^{2+}-free N-lobe. An intermediary step could here be captured in which we find CaM straddling the two termini of AC8; its C-lobe is still associated with the 1-5-8-14 motif, and its N-lobe is Ca^{2+}-saturated and bound to the IQ*lm* helix 2 (*state 2* in Fig. 9). From here, Ca^{2+}-CaM must dissociate from the 1-5-8-14 motif and bind only to the IQ*lm* (recall that $AC8_{\Delta 1-106}$ achieves maximal stimulation by Ca^{2+}/CaM). Consequent conformational changes in the whole IQ*lm* release H2 from the autoinhibitory complex, and the two termini dissociate, and disinhibition (activation) of AC8 is achieved (*stage 3* in Fig. 9). This proposal can be taken further based on a very recent report showing that of two CaM mutants (CaM_{12} and CaM_{34}, which can only bind Ca^{2+} at the C- and N-lobe, respectively), CaM_{34} can partially activate AC8 activity, whereas CaM_{12} cannot (45). This fully supports the mechanism just described, because the binding of the CaM N-lobe to H2 (wherein the critical residues for CaM association lie, as uncovered in the present study) is the first step in CaM-mediated disinhibition of AC8. *Stage 4* in Fig. 9 indicates the dissociation of CaM from the IQ*lm* after the Ca^{2+} concentration returns to basal and the re-association of CaM with the 1-5-8-14 motif. The whole system then returns to rest (Fig. 9, *stage 1*).

Overall, this study has revealed unexpected complexity in the regulation by Ca^{2+}/CaM of the IQ*lm* of AC8. Three separable events occur as follows: (i) binding of CaM; (ii) activation by CaM; and (iii) autoinhibitory events. There is a less than perfect overlap between the amino acid residues mediating these phenomena. Indeed, it appears that the IQ*lm* has a helix-loop-helix structure in which mainly hydrophobic, autoinhibitory residues are found in H1 and basic CaM-binding residues lie in H2. Although this mechanism is more elaborate than was expected, it is not dissimilar to the types of mechanisms used by CaM in regulating the activity of voltage-gated calcium channels (46, 47). Curiously, the level of mechanistic complexity suggested for AC8 is unlikely to occur with the other Ca^{2+}/CaM-stimulated AC, AC1, because this enzyme possesses only one CaMBD. Distinct physiological roles are envisaged for these functional homologues, which were recently attributed to their distinct affinities for CaM, dependences of CaM lobe Ca^{2+} occupancy, kinetics of activation, and thereby their overall dissimilarity in activation mechanism (45). The present data reinforce this assertion, because the more complex utilization of CaM by AC8 permits temporally distinguishable activation steps that could contribute to the cAMP oscillations that are seen with AC8 but not with AC1 (45, 48). Future studies may reveal yet more creative exploitation of the apparently simple motif of Ca^{2+} exerting its regulatory effects by the intercession of the ubiquitous CaM.

Acknowledgments—We are very grateful to our colleagues Nana Masada and Dr. Debbie Willoughby for careful review of the manuscript.

REFERENCES

1. Clapham, D. E. (2007) *Cell* **131,** 1047–1058
2. Berridge, M. J., Bootman, M. D., and Roderick, H. L. (2003) *Nat. Rev. Mol. Cell Biol.* **4,** 517–529
3. Bootman, M. D., Collins, T. J., Peppiatt, C. M., Prothero, L. S., MacKenzie, L., De Smet, P., Travers, M., Tovey, S. C., Seo, J. T., Berridge, M. J., Ciccolini, F., and Lipp, P. (2001) *Semin. Cell Dev. Biol.* **12,** 3–10
4. Rhoads, A. R., and Friedberg, F. (1997) *FASEB J.* **11,** 331–340
5. Shen, X., Valencia, C. A., Szostak, J. W., Dong, B., and Liu, R. (2005) *Proc. Natl. Acad. Sci. U. S. A.* **102,** 5969–5974
6. Cooper, D. M. F., Mons, N., and Karpen, J. W. (1995) *Nature* **374,** 421–424
7. Cooper, D. M. F. (1994) *Methods Enzymol.* **238,** 71–81
8. Fagan, K. A., Mahey, R., and Cooper, D. M. F. (1996) *J. Biol. Chem.* **271,** 12438–12444
9. Putney, J. W., Jr. (1986) *Cell Calcium* **7,** 1–12
10. Berridge, M. J. (1995) *Biochem. J.* **312,** 1–11
11. Smith, K. E., Gu, C., Fagan, K. A., Hu, B., and Cooper, D. M. F. (2002) *J. Biol. Chem.* **277,** 6025–6031
12. Ostrom, R. S., and Insel, P. A. (2004) *Br. J. Pharmacol.* **143,** 235–245
13. Willoughby, D., and Cooper, D. M. F. (2008) *Nat. Meth.* **5,** 29–36
14. Babu, Y. S., Sack, J. S., Greenhough, T. J., Bugg, C. E., Means, A. R., and Cook, W. J. (1985) *Nature* **315,** 37–40
15. Kretsinger, R. H., and Nockolds, C. E. (1973) *J. Biol. Chem.* **248,** 3313–3326
16. Kuboniwa, H., Tjandra, N., Grzesiek, S., Ren, H., Klee, C. B., and Bax, A. (1995) *Nat. Struct. Biol.* **2,** 768–776
17. Meador, W. E., Means, A. R., and Quiocho, F. A. (1992) *Science* **257,** 1251–1255
18. Ikura, M., Clore, G. M., Gronenborn, A. M., Zhu, G., Klee, C. B., and Bax, A. (1992) *Science* **256,** 632–638
19. Meador, W. E., Means, A. R., and Quiocho, F. A. (1993) *Science* **262,** 1718–1721
20. Osawa, M., Tokumitsu, H., Swindells, M. B., Kurihara, H., Orita, M., Shibanuma, T., Furuya, T., and Ikura, M. (1999) *Nat. Struct. Biol.* **6,** 819–824
21. Schumacher, M. A., Rivard, A. F., Bachinger, H. P., and Adelman, J. P. (2001) *Nature* **410,** 1120–1124
22. Matsubara, M., Nakatsu, T., Kato, H., and Taniguchi, H. (2004) *EMBO J.* **23,** 712–718
23. Hoeflich, K. P., and Ikura, M. (2002) *Cell* **108,** 739–742
24. Gu, C., and Cooper, D. M. F. (1999) *J. Biol. Chem.* **274,** 8012–8021

25. Ihling, C., Schmidt, A., Kalkhof, S., Schulz, D. M., Stingl, C., Mechtler, K., Haack, M., Beck-Sickinger, A. G., Cooper, D. M. F., and Sinz, A. (2006) *J. Am. Soc. Mass Spectrom.* **17,** 1100–1113
26. Simpson, R. E., Ciruela, A., and Cooper, D. M. F. (2006) *J. Biol. Chem.* **281,** 17379–17389
27. Black, D. J., Tran, Q. K., and Persechini, A. (2004) *Cell Calcium* **35,** 415–425
28. Persechini, A., and Cronk, B. (1999) *J. Biol. Chem.* **274,** 6827–6830
29. Chen, C., and Okayama, H. (1987) *Mol. Cell. Biol.* **7,** 2745–2752
30. Boyajian, C. L., Garritsen, A., and Cooper, D. M. F. (1991) *J. Biol. Chem.* **266,** 4995–5003
31. Brooks, S. P., and Storey, K. B. (1992) *Anal. Biochem.* **201,** 119–126
32. Salomon, Y., Londos, C., and Rodbell, M. (1974) *Anal. Biochem.* **58,** 541–548
33. Evans, T., Smith, M. M., Tanner, L. I., and Harden, T. K. (1984) *Mol. Pharmacol.* **26,** 395–404
34. Van Petegem, F., Chatelain, F. C., and Minor, D. L., Jr. (2005) *Nat. Struct. Mol. Biol.* **12,** 1108–1115
35. DeMaria, C. D., Soong, T. W., Alseikhan, B. A., Alvania, R. S., and Yue, D. T. (2001) *Nature* **411,** 484–489
36. Mochida, S., Few, A. P., Scheuer, T., and Catterall, W. A. (2008) *Neuron* **57,** 210–216
37. Lopez-Alcala, C., Alvarez-Moya, B., Villalonga, P., Calvo, M., Bachs, O., and Agell, N. (2008) *J. Biol. Chem.* **283,** 10621–10631
38. White, R. R., Kwon, Y. G., Taing, M., Lawrence, D. S., and Edelman, A. M. (1998) *J. Biol. Chem.* **273,** 3166–3172
39. Crossthwaite, A. J., Ciruela, A., Rayner, T. F., and Cooper, D. M. F. (2006) *Mol. Pharmacol.* **69,** 608–617
40. Vetter, S. W., and Leclerc, E. (2003) *Eur. J. Biochem.* **270,** 404–414
41. Halling, D. B., Aracena-Parks, P., and Hamilton, S. L. (2006) *Sci. STKE 2006,* er1
42. James, P., Vorherr, T., and Carafoli, E. (1995) *Trends Biochem. Sci.* **20,** 38–42
43. Tesmer, J. J., Sunahara, R. K., Gilman, A. G., and Sprang, S. R. (1997) *Science* **278,** 1907–1916
44. Cole, C., Barber, J. D., and Barton, G. J. (2008) *Nucleic Acids Res.* **36,** W197–W201
45. Masada, N., Ciruela, A., MacDougall, D. A., and Cooper, D. M. F. (2009) *J. Biol. Chem.* **284,** 4451–4463
46. Dick, I. E., Tadross, M. R., Liang, H., Tay, L. H., Yang, W., and Yue, D. T. (2008) *Nature* **451,** 830–834
47. Tadross, M. R., Dick, I. E., and Yue, D. T. (2008) *Cell* **133,** 1228–1240
48. Willoughby, D., and Cooper, D. M. F. (2006) *J. Cell Sci.* **119,** 828–836